Journal of Medicinal Chemistry

Article

Indole-2-carboxamide-Based MmpL3 Inhibitors Show Exceptional Antitubercular Activity in an Animal Model of Tuberculosis Infection

Jozef Stec, Oluseye K Onajole, Shichun Lun, Haidan Guo, Benjamin Merenbloom, Giulio Vistoli, William R. Bishai, and Alan P. Kozikowski

J. Med. Chem., **Just Accepted Manuscript** • DOI: 10.1021/acs.jmedchem.6b00415 • Publication Date (Web): 08 Jun 2016

Indole-2-carboxamide-Based MmpL3 Inhibitors Show Exceptional Antitubercular Activity in an Animal Model of Tuberculosis Infection

Jozef Stec,[d,e,#] Oluseye K. Onajole,[a,f,#] Shichun Lun,[b,#] Haidan Guo,[b] Benjamin Merenbloom,[b] Giulio Vistoli,[g] William R. Bishai,[b,c] and Alan P. Kozikowski.[a*]*

[a] Drug Discovery Program, Department of Medicinal Chemistry and Pharmacognosy, College of Pharmacy, University of Illinois at Chicago, 833 S. Wood St., Chicago, IL 60612, USA. Phone: +1-312-996-7577; Fax: +1-312-996-7107; E-mail: kozikowa@uic.edu

[b] Center for Tuberculosis Research, Department of Medicine, Division of Infectious Disease, Johns Hopkins School of Medicine, 1550 Orleans Street, Baltimore, MD 21231-1044, USA. E-mail: *wbishai1@jhmi.edu*

[c] Howard Hughes Medical Institute, 4000 Jones Bridge Road, Chevy Chase, Maryland, 20815-6789, USA

[d] Department of Pharmaceutical Sciences, College of Pharmacy, Chicago State University, 9501 S. King Drive, Chicago, IL 60628, USA

[e] Department of Pharmaceutical Sciences, College of Pharmacy, Marshall B. Ketchum University, 2575 Yorba Linda Boulevard, Fullerton, CA 92831, USA

[f] Department of Biological, Chemical and Physical Sciences, Roosevelt University, 425 S. Wabash Avenue, Chicago, IL 60605, USA

[g] Department of Pharmaceutical Sciences, Università degli Studi di Milano, via Mangiagalli 25, I-20133, Milan, Italy

Abstract

Our team had previously identified certain indolecarboxamides that represented a new chemical scaffold that showed promising anti-TB activity both at an *in vitro* and *in vivo* level. Based on mutational analysis using bacteria found resistant to one of these indolecarboxamides we identified the trehalose

monomycolate transporter MmpL3 as the likely target of these compounds. In the present work we now further elaborate on the SAR of these compounds which has led in turn to the identification of a new analog, 4,6-difluoro-*N*-((1*R*,2*R*,3*R*,5*S*)-2,6,6-trimethylbicyclo[3.1.1]heptan-3-yl)-1*H*-indole-2-carboxamide (**26**), that shows excellent activity against drug-sensitive (MIC = 0.012 μM; SI ≥16000), multidrug-resistant (MDR), and extensively drug-resistant (XDR) Mtb strains; has superior ADMET properties, and that shows excellent activity in the TB aerosol lung infection model. Compound **26** is also shown to work in synergy with rifampin. Because of these properties, we believe that indolecarboxamide **26** is a possible candidate for advancement to human clinical trials.

Keywords: tuberculosis, indole-2-carboxamide, drug resistance, MmpL3 transporter, homology modeling, aerosol infection model

Introduction

Tuberculosis (TB) is an airborne infectious disease caused by *Mycobacterium tuberculosis* (Mtb) that predominantly affects the lungs. Statistics show an inexorable increase in global health problems and socioeconomic burden brought about by TB worldwide. The regions consisting of South-East Asia, the Western Pacific, and Africa are the most impacted, and in 2014 accounted for nearly 86% out of the estimated 9.6 million new TB cases.[1] Given the fact that TB predominantly occurs among men (over 60% of TB cases and deaths due to TB) during their economically most productive years, the economic loss in productivity due to TB is predicted to be 1-3 trillion dollars over the next 10 years.[2] Major challenges that prevent the eradication of TB include the inappropriate use or overuse of prescribed medications, inadequate diagnosis and failure to adhere to the required drug regimen, as well as financial factors that may preclude access to the required medicines. Moreover, the improper use of TB antibiotics has led to the emergence of multidrug-resistant (MDR) and extensively drug-resistant (XDR) TB. An estimated

317,000 (~3.3%) of new TB cases in 2014 were identified as MDR-TB. Among those patients with MDR-TB, approximately 31,000 (~ 9.7%) were found to be infected with XDR-TB.[1]

The current TB drug pipeline includes several chemical entities representing various known and novel chemical scaffolds that interfere with the function of molecular targets operating within essential metabolic pathways such as cell envelope biosynthesis, nucleic acid and protein synthesis, and membrane energy production/transport.[3] These chemical entities are currently being evaluated at various stages spanning from preclinical development to Phase III clinical trials.[4] Of special importance is the approval of bedaquiline by the U.S. Food and Drug Administration in December 2012,[5] as well as delamanid and *para*-aminosalicylic acid by the European Medicines Agency in November 2013.[6] All three drugs were approved for combination therapy against pulmonary MDR-TB infections when other effective treatment options are not useful due to resistance or tolerability. However, as with many known anti-TB drugs, the use of bedaquiline is accompanied by various adverse effects with irregular heart rhythm being the most pronounced.[7] Thus, the need for safe, highly effective, and fast acting anti-TB drugs with novel modes of action cannot be overemphasized.

The elucidation of essential molecular targets within Mtb and the elaboration of novel chemical scaffolds possessing desirable physicochemical and ADME/Tox properties are at the forefront of the discovery and development pipeline to identify better antitubercular therapeutics. Recently, MmpL3, a protein that belongs to the resistance, nodulation and cell division (RND) family of membrane transporters has been identified as a druggable molecular target essential for Mtb's survival.[8] MmpL3, encoded by the *Rv0206c* gene, is a large protein anchored in the inner lipid bilayer that is comprised of 11 transmembrane helices, two extracellular domains (E1, E2), and one intracellular domain (C1).[9] MmpL3 is responsible for translocation of mycolic acids in the form of trehalose monomycolate (TMM) from their production site in the cytoplasm into the cell envelope. Subsequently TMM is processed in the extracytoplasmic space by mycolyl transferases of the antigen 85 complex, which transfer the lipid portion of TMM to another TMM molecule to afford trehalose dimycolate (TDM), or to arabinogalactan yielding wall-bound mycolates.[10]

The released trehalose is recycled by ATP-binding cassette transporters (LpqY-SugA-SugB-SugC), a process known to be essential for the virulence of Mtb.[11] The arabinogalactan-bound mycolates are long α-branched β-hydroxy fatty acids that make up the thick, waxy, and difficult-to-permeate outer coating of the bacterial envelope.[12] Accordingly, inactivation of the MmpL3 transporter prevents the translocation of the mycolic acids to the outer layer thus weakening the bacterial cell wall and impacting the viability and virulence of Mtb. Additionally, other recent studies reveal that MmpL3 along with another family member MmpL11 play a role in the transport of heme-iron.[13] The precise extent to which MmpL11 and MmpL3-mediated iron uptake contribute to TB virulence is still under study.[9] Lastly, a more recent paper has provided evidence that a number of the MmpL3 inhibitors may actually work by causing the dissipation of the proton motive force that is required for the function of MmpL3 and other MmpL-driven processes.[14]

In our previous work, based on phenotypic screening, we identified the indole-2-carboxamide **1** as a highly potent scaffold against drug-susceptible and drug-resistant Mtb strains (Figure 1).[15] Employing a standard medicinal chemistry approach, a number of analogs were made which lead to compound **3** that was found to show superior activity against susceptible, MDR and XDR Mtb strains in comparison to **1**.[15] Using genome sequencing methodology we also determined that compound **3** targets the MmpL3 transporter protein which has consequences for the viability of Mtb as detailed above.[16] Herein we report further SAR studies on these indolecarboxamides, together with *in vitro* pharmacokinetic (PK) analysis as well as *in vivo* TB mouse efficacy studies for the best of these new indoles. These data point to compound **26** as a possible candidate for further advancement through the development pipeline.

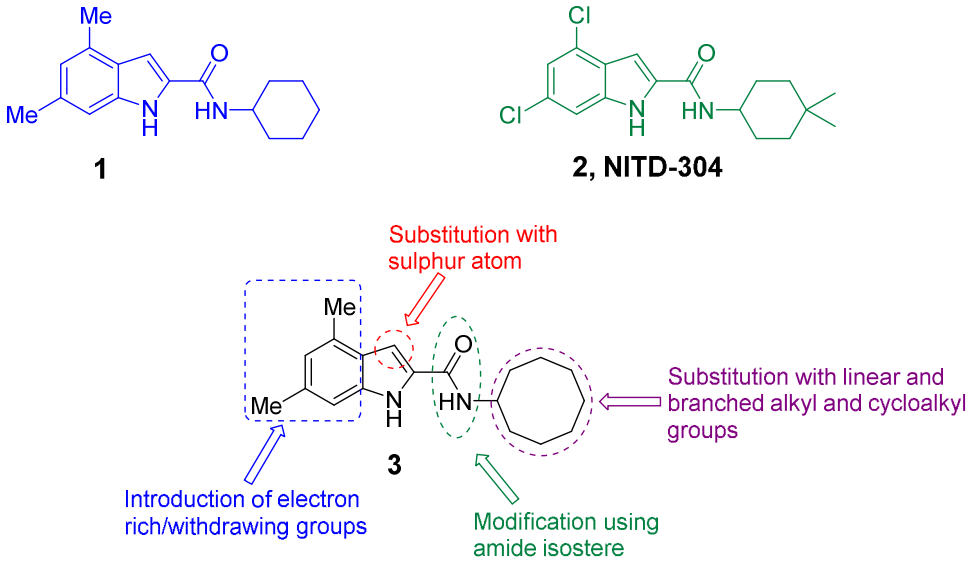

Figure 1. Hit compound **1,** lead compounds **2** and **3**, and strategy for additional chemical modifications of the indole-2-carboxamide scaffold **3**.

Results

Following the amide coupling protocol (Scheme 1), 40 novel indolecarboxamides and related compounds were efficiently generated. Briefly, the substituted indole-2-carboxylic acids were reacted under an argon atmosphere with an alkyl- or cycloalkylamine in the presence of 1-ethyl-3-(3-dimethylaminopropyl)carbodiimide hydrochloride (EDC·HCl) and hydroxybenzotriazole (HOBt) as coupling agents and triethylamine as a base to obtain compounds **3**–**39** (Scheme 1). To prepare compounds **6** and **9**, the starting materials **52** and **53** were reacted with cyclooctylamine under standard amide coupling conditions followed by catalytic hydrogenation of the nitro groups (Scheme 1). To prepare intermediate **55**, 3,5-dimethoxyaniline (**54**) was reacted with ethyl bromoacetate to afford ethyl 2-[(3,5-dimethoxyphenyl)amino]acetate which was reacted in turn with *N*,*N*-dimethylformamide dimethyl acetal (DMFDMA) under microwave irradiation. Next, Lewis acid ($AlCl_3$)-promoted cyclization of **55** afforded the cyclized indole-2-carboxylate, which after basic hydrolysis gave the corresponding acid **56**.

The indole carboxylic acid **56** was reacted with cycloheptylamine and cyclooctylamine to afford compounds **18** and **19**, respectively.

4,6-Dimethyl-1*H*-indole-2-carboxylic acid (**43**)[15] (Scheme 2) was reacted with ammonium chloride to afford compound **57**, which was reduced to its corresponding primary amine and reacted with cycloheptanecarbonyl chloride to afford compound **40**. The amide group of compound **3**[15] was reduced to the corresponding amine **41**. The benzothiazole analog **42** was obtained from the benzo[*d*]thiazol-2-amine **58** by reaction with cycloheptanecarbonyl chloride (Scheme 2).

Scheme 1. [a] Synthesis of indole-2-carboxamides

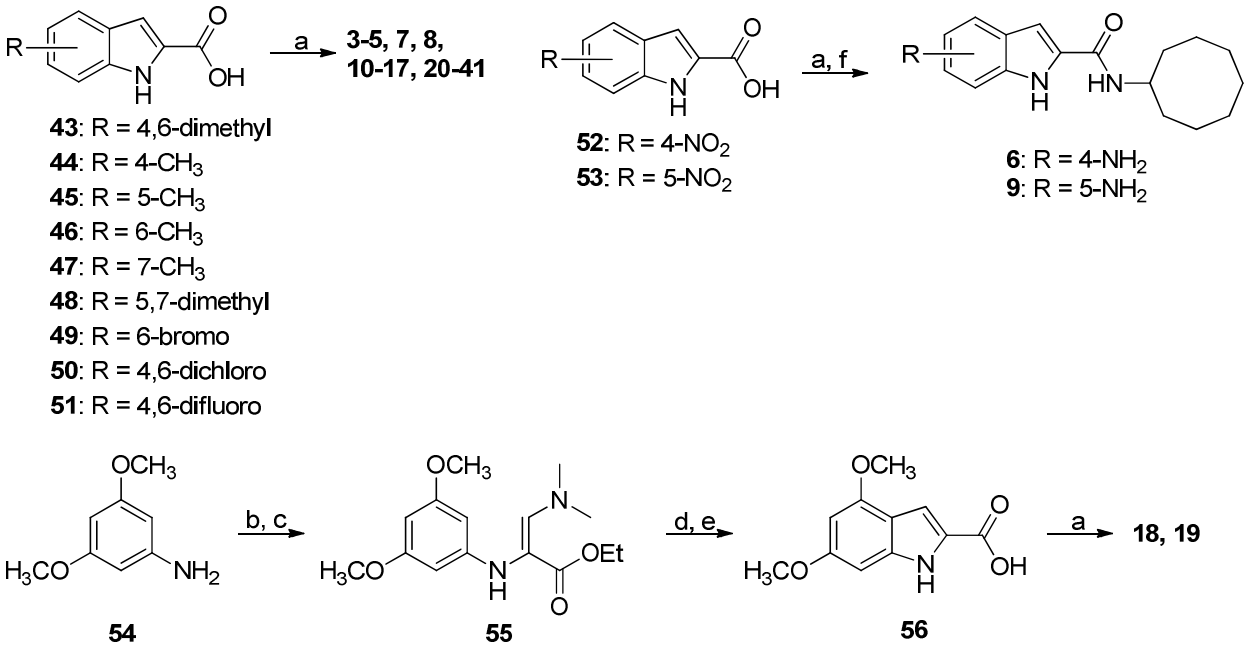

[a]Reagents and conditions: (a) EDC·HCl, HOBt, corresponding amines, Et_3N, CH_2Cl_2, rt, 12–16 h; (b) ethyl bromoacetate, K_2CO_3, acetone, 60 °C, overnight; (c) DMFDMA, microwave, 150 °C, 10 min; (d) $AlCl_3$, CH_2Cl_2, 24 h, rt; (e) LiOH, EtOH, reflux, 3 h; (f) 10% Pd/C, MeOH/EtOAc (4:1), H_2.

Scheme 2.[a] Synthesis of analogs containing indole and benzothiazole skeleton

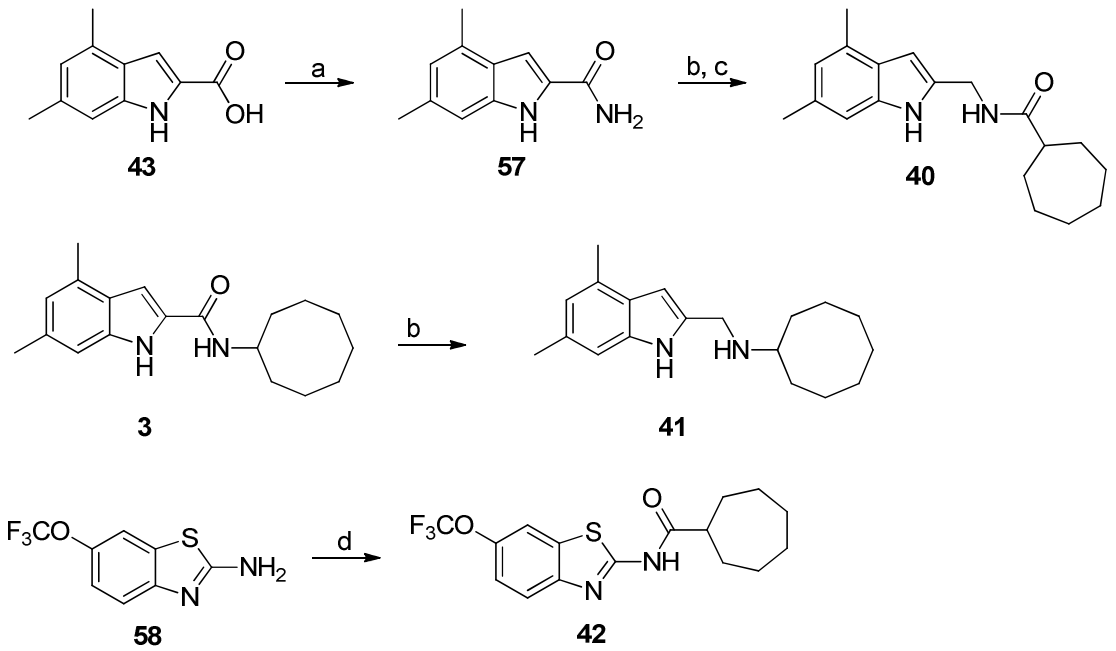

[a]Reagents and conditions: (a) EDC·HCl, HOBt, NH_4Cl, Et_3N, CH_2Cl_2, rt, 12–16 h; (b) $LiAlH_4$, THF, reflux, overnight; (c) EDC·HCl, HOBt, cycloheptanecarboxylic acid, Et_3N, CH_2Cl_2, rt, 12–16 h; (d) cycloheptanecarbonyl chloride, CH_2Cl_2, rt, overnight.

Discussion and Conclusions

Structure-Activity Relationships

In general, the biological activity of the analogs was found to depend upon the polarity of the substituents introduced, and thus the more lipophilic compounds were found to be the most active. Compounds possessing mono-substitution such as a methyl group at position 4 of the indole moiety (**4**, **5**) retained antitubercular activity, with compound **5** bearing the *N*-cyclooctyl group being over 8-fold more active than its closest analog **4** bearing the *N*-cycloheptyl group. On the other hand, the more polar 4-aminoindole derivative **6** showed inferior activity. A similar trend in activity was observed for compounds **7**-**9** possessing methyl or amino substitution at position 5 of the indole ring. However, these compounds were consistently less potent than their corresponding counterparts **4**-**6** which further

confirms the lipophilicity-driven activity of these analogs but also indicates that position 4 is preferred for functionalization. In the case of position 6, mixed results were obtained as compound **11** bearing the more lipophilic bromo group was only slightly more active than its close analog **10** possessing the 6-methyl group. On the other hand, compound **12** bearing an *N*-adamantyl group was 2.6- and 2-fold more active than compounds **10** and **11,** respectively, although has a ClogP comparable to that of **10**, which is lower than that of analog **11**. In line with the activity of the adamantyl derivative, we were also interested in evaluating bicyclic substituents. Our attention was drawn to the pinene skeleton as this structure is known for its broad antimicrobial activity.[17] It was pleasing to find that compound **13** bearing the *N*-(*1R*,*2R*,*3R*,*5S*)-(-)-isopinocampheyl group is 4-fold more active than compound **12** and 9-fold more active than analog **11**. Again, compound **13** is the most lipophilic molecule among compounds **10**-**13** supporting the requirement of high lipophilicity for bioactivity. To complete the investigation of the effect of mono-substitution of the indole ring on activity, a methyl group was installed at position 7 in compounds **14** and **15**. As observed earlier for compound pairs **4**/**5** and **7**/**8**, compound **15** bearing the *N*-cyclooctyl group was more active than its counterpart **14** possessing the *N*-cycloheptyl substituent.

Next, we examined the effect of di-substitution with methyl and methoxy groups on the indole ring. As expected, the *N*-cyclooctyl indoles **17** and **19** were more active than their *N*-cycloheptyl counterparts (**16** and **18**). Surprisingly, the 4,6-dimethoxy compounds (**18** and **19**) had almost the same activity as the 5,7-dimethyl analogs (**16** and **17**), although the latter pair has higher ClogP values than compounds **18** and **19**, respectively. Knowing that biological activity of this series of compounds is lipophilicity-driven and that the methyl groups on the indole core present a potential metabolic liability (susceptible to metabolic oxidation),[16] we replaced the 4,6-dimethyl substituents with more lipophilic and at the same time metabolism-resistant 4,6-dihalo-groups.[18] Compound **20** containing a 4,6-dichloro-indole scaffold was the first to be prepared, and this analog showed similar activity as the lead compound **3**. Derivative **21** bearing the *N*-adamantyl group was equally potent as compound **20**, although its ClogP value is lower than that of **20**. Another structurally close analog **22** bearing the *N*-*exo*-2-norbornyl substituent showed a

greater than 30-fold drop in activity when compared to **20**. This result is most likely associated with the substantial difference in lipophilicity observed between the two molecules. Introduction of the *N*-(*R*)-(+)-bornyl group provided compound **23** which was 9-fold more potent than **22** but approximately 4-fold less active than **20**. Interesting results were obtained with compounds **24**-**27** which bear an isopinocampheyl moiety on the amide nitrogen atom. The 4,6-dichloroindole nucleus with the *N*-(*1R*,*2R*,*3R*,*5S*)-(-)-isopinocampheyl group **24** proved to be 2-fold more active than compound **23** but also was approximately 2-fold less active than compound **20** having the *N*-cyclooctyl group. Of note is the fact that compound **24** is more lipophilic than **20** and has the same ClogP value as molecule **23**. On the other hand, the *N*-(*1S*,*2S*,*3S*,*5R*)-(+)-isomer **25** turned out to be 2-, 4-, and 7-fold less potent compared to indoles **23**, **24**, and **20**, respectively. Given the fact that all three compounds **23**-**25** have the same ClogP values, it is apparent that the stereochemical orientation of the amide nitrogen substituent plays some role in the biological activity of this series of compounds. Even more pronounced results were obtained for the pair of enantiomers **26** and **27** possessing the 4,6-difluoro indole scaffold. In this case, the dextrorotatory isomer **27** was nearly 16-fold less potent than the levorotatory isomer **26** while the latter showed about the same potency as **20** and about a 2-fold improvement in activity compared to **24**. This is a noteworthy result as the lipophilicity of compound **26** is lower that of analogs **20** and **24**, yet it shows an *in vitro* antitubercular potency comparable to that of **20**. Based on their satisfactory *in vitro* activity, all three compounds, i.e. **20**, **24**, and **26** were selected for further *in vivo* studies in the serum inhibitory titer assay (SIT).

Appendage of a simple *n*-heptyl or *n*-octyl aliphatic chain on the amide nitrogen yielded the highly lipophilic compounds **28** and **29**, but surprisingly these were nearly inactive. These findings clearly support the importance of a more compact, α-branched cycloaliphatic group on the amide nitrogen in order to observe high activity. Compounds **30** and **31** containing the *N*-geranyl moiety provided mixed results with compound **30** possessing inferior activity and compound **31** being inactive. Compounds **30** and **31** depict once again the apparent impact of lipophilicity on activity. The β-branched *N*-substituent in

compound **32** also led to loss of activity while a similar alpha-branched *N*-substituent gave the reasonably active compound **33** and the modestly active compound **34**. This result clearly supports the importance of a lipophilic branched cycloaliphatic group for the bioactivity as it is likely to be more resistant to metabolism than the non-branched substituents. Compound **35** with a 5,6-fused amide substituent retained activity. On the contrary, compound **36** possessing the same *N*-substituent as **35** turned out to be inactive most likely due to a drastic decrease in lipophilicity. The spiro compounds **37** and **38** provided the highest *in vitro* antitubercular activity identified in this set of compounds. Given their high potency, these compounds were also selected for *in vivo* SIT assay. The azabicylic compound **39** bearing a tertiary amine showed a significant decrease in activity. Furthermore, compound **40** featuring a reversed amide linker, and the benzothiazole derivative **42** were inactive against a susceptible strain of Mtb. Reduction of the amide group of **3** to obtain the amine **41** resulted in a 24-fold drop in TB activity thus highlighting the importance of the carboxamide linker for anti-TB activity.

Overall, the SAR for this set of compounds is complex with several factors being decisive for high antitubercular activity. The indole nucleus possessing 4,6-disubstitution with lipophilic groups is crucial for activity. Halogen substituents such as F or Cl are preferred over methyl groups, which may constitute a metabolic liability. Carbocyclic groups with an alpha-branched carbon on the *N*-indolecarboxamide atom yielded the best compounds. The dependence of activity on the absolute configuration of this substituent suggests that it may be involved in specific interactions with the target, rather than just enhancing the compound's lipophilicity.

Table 1. MIC and ClogP values of indole-2-carboxamides analogs.

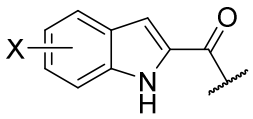

3-39

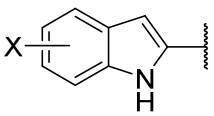

40-41

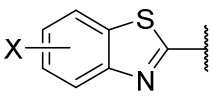

42

Analog	X	R	MIC[a]	ClogP[b]	Analog	X	R	MIC[a]	ClogP[b]

			(μM)					(μM)	
3	4,6-dimethyl	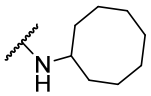	0.013	5.59	**24**	4,6-dichloro	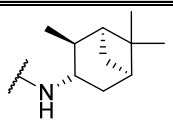	0.021	6.88
4	4-methyl	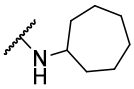	0.93	4.54	**25**	4,6-dichloro	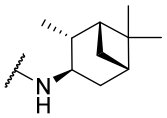	0.086	6.88
5	4-methyl	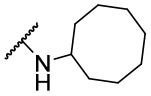	0.11	5.10	**26**	4,6-difluoro	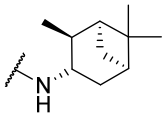	0.012	5.74
6	4-amino	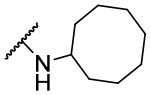	20	3.44	**27**	4,6-difluoro	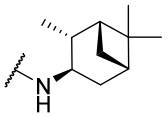	0.19	5.74
7	5-methyl	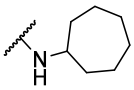	7.4	4.54	**28**	4,6-dichloro	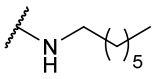	>300	6.19
8	5-methyl	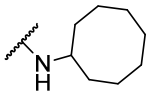	0.88	5.10	**29**	4,6-dichloro	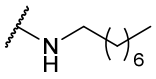	>300	6.72
9	5-amino	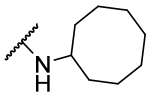	80	3.44	**30**	4,6-dichloro	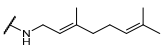	11	6.75
10	6-methyl	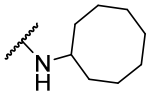	0.11	5.10	**31**	4,6-difluoro	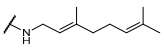	>192	5.61
11	6-Br	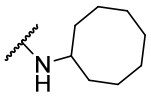	0.09	5.56	**32**	4,6-dichloro	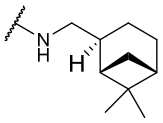	175	6.98
12	6-Br	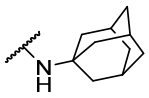	0.042	5.07	**33**	4,6-dichloro	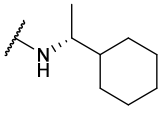	5.9	5.97
13	6-Br	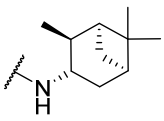	0.010	6.28	**34**	4,6-difluoro	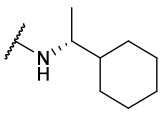	13	4.83

14	7-methyl	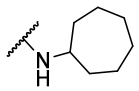	30	4.54	**35**	4,6-dichloro	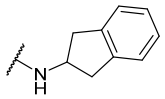	0.72	5.00
15	7-methyl	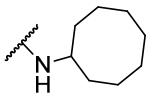	3.5	5.10	**36**	4,6-difluoro	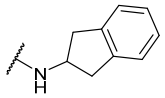	102	3.86
16	5,7-dimethyl	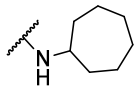	3.5	5.04	**37**	4,6-dichloro	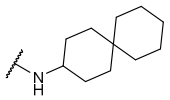	0.005	7.04
17	5,7-dimethyl	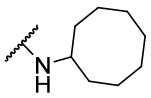	0.21	5.59	**38**	4,6-difluoro	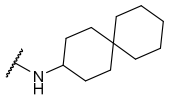	0.003	5.90
18	4,6-dimethoxy	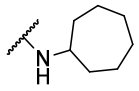	3.2	4.01	**39**	4,6-dichloro	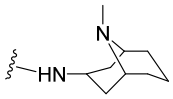	10.9	3.94
19	4,6-dimethoxy	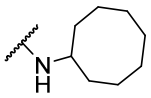	0.19	4.57	**40**	4,6-dimethyl	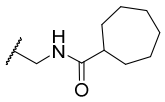	54	4.53
20	4,6-dichloro	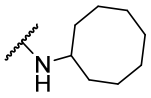	0.011	6.16	**41**	4,6-dimethyl	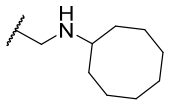	0.31	5.65
21	4,6-dichloro	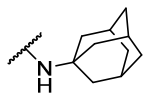	0.011	5.67	**42**	5-trifluoro-methoxy	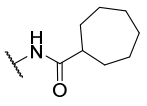	>300	4.47
22	4,6-dichloro	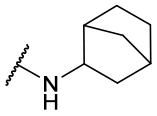	0.39	5.32	**INH**[c]			0.29	
23	4,6-dichloro	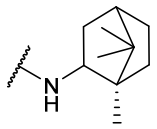	0.043	6.88					

[a]The lowest concentration of drug leading to at least a 90% reduction of bacterial growth signal by the microplate alamarBlue assay (MABA). MIC values are reported as an average of three individual measurements; [b]Calculated using ChemBioDraw Ultra 13.0; [c]INH = Isoniazid.

In vivo Bioavailability and _in vitro_ Activity of Selected Indole-2-carboxamides against Clinical Isolates of Mtb.

The most promising compounds in this series, namely **20**, **21**, **24**, **26**, **37**, **38**, and the comparator compound **2** reported by Novartis[19] (prepared in-house) were further evaluated for their *in vivo* bioavailability in the serum inhibition titration (SIT) assay (Figure 2).[20] As depicted in Figure 2, compound **24** showed much higher bioavailability and thus *in vivo* efficacy when compared to **2** and **20**, but it was less effective than the reference drug isoniazid. On the other hand, compound **26** showed excellent *in vivo* efficacy that was comparable to that of isoniazid when tested at a dose of 100 mg/kg. Compound **26** also showed significant improvement in bioavailability when compared to the lead compound **3** (results not shown).[15] The other compounds selected for SIT analysis, namely **21**, **37**, and **38** turned out to be inactive (results not shown) in this assay and thus there were dropped from further studies.

Based on their activity in the SIT screening assays, compounds **20**, **24**, and **26** were next tested against a panel of clinical isolates[21] of Mtb originally obtained from pulmonary TB patients (Table 2). Among those strains, one was drug-sensitive (DS) (V4207), two were MDR Mtb (KZN494, V2475), and two were XDR Mtb (TF274, R506). Compound toxicity against mammalian cells was tested on Vero cells and a selectivity index (SI) subsequently calculated (Table 2). All three compounds retained their high activity or showed only a moderate (up to 4- and 8-fold for **26** and **24**, respectively) decrease in activity against the tested clinical isolates of Mtb. Of note is the fact that compounds **20** and **26** showed a 2-fold increase in activity against the XDR Mtb strains R506 and TF274, respectively. The high activity of these compounds against MDR and XDR TB indicates not only their potential to treat drug-resistant Mtb strains but also suggests the likelihood that these compounds will not exhibit cross-resistance with currently used medications. Additionally, all the three compounds exhibited high IC_{50} values against Vero cells, thus resulting in high SI indices, and thus indicating their potential lack of toxicity toward

mammalian cells. We also tested **26** against the TSK54R mutant which we had generated in our initial studies and used in the DNA deep sequencing efforts to identify MmpL3 as the target of the indolecarboxamides. The MIC was 0.0625-0.125 μg/mL, which corresponds to a 16-32-fold loss of activity against the mutant indicating MmpL3 as the potential target. Based on its excellent *in vitro* activity, superior SI, and high efficacy in the SIT assay, compound **26** was selected for further development.

Table 2. Activity [MIC (μM)] of indole-2-carboxamides against selected clinical isolates of Mtb and Vero cells [IC_{50} (μM)].

Strain	H37Rv	V4207	KZN494	V2475	TF274	R506	IC_{50}	SI[d]
Phenotype	DS	DS	MDR[a]	MDR[a]	XDR[b]	XDR[b]	Vero Cells	
20	0.011	0.011	NA[c]	0.011	0.011	0.006	23.5-47	2136-4272
24	0.021	0.043	0.043	0.171	0.021	0.021	43.8	2085
26	0.012	0.023	0.012	0.047	0.006	0.012	≥192	≥16000

[a] Resistance to isoniazid and rifampin; [b] Resistance to isoniazid, rifampin, levofloxacin, ofloxacin, and kanamycin; [c] Data not available due to growth defect; [d] Selectivity Index (SI) = $IC_{50\ (Vero)}$ / MIC

Preliminary ADMET Studies on Compound 26.

Based on the encouraging biological results described above, we conducted some ADMET studies on compound **26** to assess its drug-like properties (Table 3). When incubated with human, mouse, rat or dog liver hepatocytes, at least 50% of compound **26** remains unchanged after 2 hours incubation using a starting concentration of 1 μM and the human hepatocytes. More substantial degradation was found using hepatocytes from the other species. Using liver microsomes, almost 70% of the compound remained unchanged after 1 hour using a starting concentration of 3 μM.

Table 3. ADMET data for indole-2-carboxamide 26.

Assay	**26**
Hepatocytes, % remaining at 2 hrs, starting concentration 1 μM	52 (human), 0.7 (rat), 15 (mouse), 18 (dog)
Liver microsomes, % remaining after 1 hr, starting concentration 3 μM	69.5 (human, 60 mins)
CYP inhibition (% inhibition)	
CYP2C9	-5.2
CYP2D6	36.6
CY3A4	-6.7
Caco-2 permeability	
A-B (cm/s)	0.19×10^{-6}
B-A (cm/s)	0.25×10^{-6}
hERG IC_{50} (μM)	>30

As shown in Table 3, in the presence of compound **26** none of the tested CYP isoforms (CYP2D6, CYP2C19, and CYP3A4) showed more than 40% inhibition. Low inhibition of hERG (IC_{50} > 30 μM) suggests low potential risk for blocking the cardiac calcium channel and causing QT-prolongation. As the xenobiotic-sensing transcription factors that include the pregnane X receptor (PXR), aryl hydrocarbon receptor (AhR), and the constitutive androstane receptor (CAR) upregulate the expression of drug-metabolizing genes (CYP3A4, CYP1A2 and CYP2B6, respectively), the potential of **26** to cause transactivation of the human PXR, CAR, and AhR receptors was assessed. At low concentrations of the compound tested (0.1-1 μg/mL), no significant induction of the respective reporter genes coupled to these

nuclear receptors was observed. Only at higher concentrations (3 and 8 μg/mL) was **26** able to upregulate the induction of metabolizing genes by these receptors. However, the levels of induction produced by **26** were still lower than those of the positive controls, i.e. rifampin for PXR, CITCO for CAR, and 3-methylcholanthrene for AhR. We also carried out the bacterial reverse mutation assay in *Salmonella typhimurium* tester strains TA98, TA100, TA1535, and TA1537 and *Escherichia coli* tester strain WP2 uvrA for compound **26** to evaluate its intrinsic mutagenic activity, and for the most part these results were negative. Only in the case of the TA98 tester strain with the S9 liver fraction present was an increase in the ratio of the revertant colony count for the drug compared to the DMSO solvent control observed. This ratio was 2.5 with 500 μg/plate of drug. Even at 5000 μg/plate of the **26** this ratio was only 2.0 whereas this ratio was 173 for the positive control 2-aminoanthracene. Thus we believe the genotoxicity risk of this compound to be negligible although further studies to detect chromosomal aberrations should be done.

Pharmacokinetic comparisons of 26 and 2 using LC-MS. Next, we carried out comparative pharmacokinetic studies on **26** and the comparator compound **2** using traditional liquid chromatography-mass spectrometry (LC-MS) analysis (Table 4). A single dose of 100 mg/kg was administered orally to female Balb/c mice. As shown in the table below, **26** showed significantly better PK parameters than **2** as reflected by higher AUC_{last} (area under the curve up to the last measurable concentration) and higher $AUMC_{last}$ (area under the first moment curve to the last measurable concentration; this is a measure of AUC which emphasizes mean residence time).

Table 4. Pharmacokinetic comparisons of compounds **2** and **26.**

Compound		T_{MAX} (h)	C_{MAX} (μg/unit)	AUClast (h•μg/unit)*	AUMClast (h^2•μg/unit)*	MRTlast (h)

26	Plasma	4	1.71	18.9	137	7.28
	Lung	4	3.50	51.0	433	8.49
2	Plasma	2	0.67	5.62	36.4	6.47
	Lung	2	1.30	18.1	150	8.30

*unit = mL for plasma samples; unit = gram for lung samples; AUMC = area under the first moment curve; MRT = mean residence time.

Mouse efficacy comparisons of 26 and 2. Lastly, we completed *in vivo* efficacy studies for **26** and **2** using two different mouse infection and monotherapy models. In order to enable head-to-head comparisons, we deliberately used 0.5% carboxymethylcellulose (CMC) for both of the test compounds although we are aware that more advanced formulations are now available. A minimum effective dose (MED) model was conducted using Balb/c mice that had been aerosol-infected and treated from day 1 at 12.5, 25, 50 and 100 mg/kg for both compounds. While both compounds were protective, **26** showed more obvious dose-dependent effects than **2** on both CFU enumerations in the lungs (Figure 3) and gross pathology such as lung weight and spleen weight. For comparison, at 100 mg/kg dosage level, there was a CFU reduction of 1.71- and 2.12-log in the lungs after treatment with **26** for 2 weeks and 4 weeks, respectively. For **2**, the CFU reduction was 0.45- and 1.08-log for the same dosage level and treatment durations, respectively (p<0.0001). A minimum bactericidal dose (MBD) model was also carried out. After 4 weeks of treatment at 200 mg/kg, **26** achieved 0.6-log CFU reduction while **2** left the CFU count unchanged compared with that of initiation (p=0.0002). All treatment levels (25, 50, 100 and 200 mg/kg) of both indolecarboxamides protected mice from death. In these studies, we used the universal formulation, which is 0.5% carboxymethylcellulose in water. The universal formulation used in this study differs from the optimized customized proprietary formulation used by Novartis, which in turn might have contributed to the observed difference in the efficacy between compound **26** and **2** in mice model.

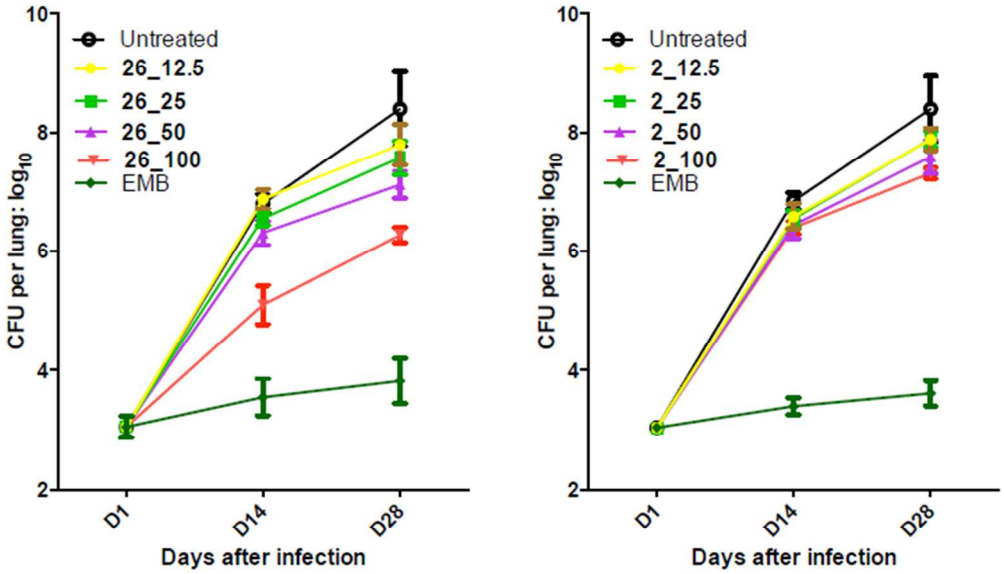

Figure 3. In vivo efficacy comparisons of compounds 26 and 2 in a mouse infection model. After aerosol *Mtb* infection with 10^3 CFU, mice were treated orally with 12.5, 25, 50, and 100 mg/kg of **26** or **2** daily. EMB was at 100 mg/kg/d. Lung CFU counts were determined on days 1, 14, and 28 (5 mice/grp).

***In vitro* and *in vivo* Synergy between Indole-2-carboxamide 26 and Rifampin.**

Previous studies suggested that mutation in the *mmpL3* gene confers increased susceptibility of Mtb to rifampin [22]. Since indolecarboxamides target a molecular channel, we hypothesized that the antibacterial effect of dual exposure to indolecarboxamide and rifampin might meet the criteria for true synergy rather than being two independent, additive effects. To address this question, we applied the Bliss independence model which evaluates multiplicative effects in growth measures and has been used extensively in evaluating pharmacologic drug-drug interactions.[23] As shown in Table 5, Bliss synergy was observed in multiple sub-MIC concentration combinations as highlighted. For instance, 0.5×MIC of **26** combined with 0.0313×MIC of rifampin achieved 99.2% inhibition (MIC cutoff = 90%). Similarly, 0.25× or 0.0313×MIC of **26** plus 0.25× or 0.5×MIC of rifampin also achieved MIC level of inhibition (99.4% or 90.5% respectively, Table 5). Rifampin is a key component of multidrug TB therapy and is considered

particularly important for clearance of *M. tuberculosis* persisters and to achieving a relapse-free cure in six-months. However, rifampin is a potent inducer of both cytochrome P-450 oxidative enzymes and the P-glycoprotein transport system.[24] Because of these interactions, dose adjustments are necessary when rifampin is used with numerous drugs including warfarin, contraceptives, cyclosporine, quinidine sulfate, and verapamil, to name a few.[24b, 25] Importantly, rifampin also interacts with HIV-related protease inhibitors and significantly reduces the concentration of many standard-dose protease inhibitors, compromising HIV treatment efficacy.[26] Our findings of synergy between **26** and rifampin are important because it raises the possibility that indolecarboxamide-containing treatment regimens with lower rifampin doses could be efficacious. Reduced rifampin exposures could be especially important for patients with HIV/TB co-infection who require anti-retroviral therapy.

Table 5. *In vitro* drug combination of indole-2-carboxamide 26 and rifampin.

		Compound 26							
		0.0313	0.0625	0.125	0.25	0.5	1.0	2.0	4.0
Rif	4.0								
	2.0								
	1.0								
	0.5	0.0	0.1	0.1	0.1	0.1			
	0.25	0.1	0.1	0.4	0.6	0.6			
	0.125	0.1	0.1	0.1	0.8	1.0			
	0.0625	0.0	0.0	0.0	0.1	1.0			
	0.0313	0.0	0.0	0.0	0.0	1.0			

Note: Checkerboard synergy study showing the calculated effect of the combination of **26** combined and rifampin. Bliss independence modeling was applied to wells containing < 1×MIC concentration of either compound. Synergy (Δf_{axy} >0) was observed in multiple combinations and highlighted.

Most interestingly, in an acute mouse infection and chemotherapy model, treatment with a combination of **26** and rifampin achieved synergistic effects, as evaluated using the Bliss synergy model (Figure 4). This implies a great potential for indolecarboxamide **26** and analogs to be used in the standard regimen for shortening the duration of TB treatment.

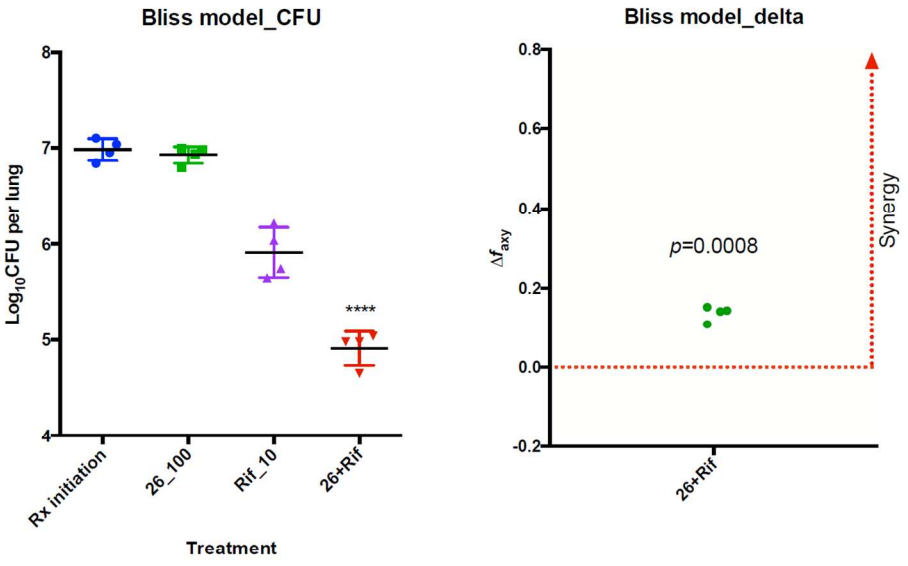

Figure 4. Bliss synergy model using rifampin and **26**. Compound **26** synergizes with rifampin in an acute mouse infection and chemotherapy model.

Molecular Docking of Compound 26 and Related Indole-2-carboxamides

In order to gain some understanding of how the indolecarboxamides interact with the MmpL3 transporter, we constructed a possible model of the transporter using methods provided in the supplemental section. As shown in Figure 5, the overall folding of the MmpL3 transporter is characterized by a complex TM bundle, including 12 TM helices, and two large periplasmic domains: the first domain (D1) is located between TM1 and TM2 and the second (D2) between TM7 and TM8. Compared to the selected template (MexB transporter, see Table S1 in SI), MmpL3 conserves the two periplasmic domains which define the so-called pore domain and are characterized by β–α–β motifs, while it lacks the so-called docking domains (DN and DC) which are usually involved in contacting modulating proteins. The overall folding can be divided into two halves, each composed of six TM helices and one periplasmic domain. The two halves are connected by an intracellular helical domain (D3). Figure 5 also shows the bound compound **3** thus revealing the location of the putative binding pocket which is on the cytoplasmic side of the TM bundle mostly lined by TM4 and TM10.[27]

Moreover, since the considered template (MexB transporter) includes an asymmetric homotrimer where each subunit adopts a different conformation which may represent snapshots of the transport process, it is worth noting that the monomer utilized as the template is the so-called binding monomer (monomer B) since the *n*-dodecyl-D-maltoside (DDM) ligand is bound in the cavity defined by its periplasmic domains and the channel is open to the periplasm from which it can capture the substrates. Although the considered pocket for the inhibitors does not correspond to that lined by the periplasmic domains, one may conjecture that the generated homology model (for details see Table S1 in SI) would be in a conformation suitable to investigate the binding of the transported substrates. Notably, the last discarded MmpL3 model (model #5, Table S1 in SI) was generated by using the so-called extrusion monomer (monomer C) of its template, which shows a wider TM bundle to allow the substrate release. This may explain why the pocket of model #5 is clearly wider and suggests that this cavity, albeit less functional,

can be seen as an alternative binding conformation that the transporter can assume during the transport cycle.

Figure 5. Cartoon structure of the MmpL3 homology model as colored by N (blue) to C (red) sequence. The bound inhibitor **3** is also depicted as the grey-colored CPK model.

Figure 6A shows the main interactions stabilizing the putative complex between the MmpL3 model and **3**, which can be schematized as follows. The first subpocket accommodates the indole ring which elicits an extended charge transfer interaction with Arg259 reinforced by π–π stacking with Phe644 plus a set of hydrophobic contacts with surrounding apolar residues such as Ile256, Val278, Ala281, Val285, and Pro330. Moreover the indole NH group stabilizes a H-bond with Ser325. A central subpocket stabilizes a rich set of H-bonds with the ligand's amide moiety: the carbonyl oxygen atom contacts Tyr252, Ser288, and Ser325, while the amide NH group interacts with Asp640 which in turn establishes an ion-pair with

the above-cited Arg259. Notably, Tyr252 is highly conserved among the MmpL isoforms and is adjacent to another residue (Gly253), the mutation of which was found to decrease the inhibition activity of known MmpL3-targeting compounds such as SQ109 and AU1235. Again, Arg259 and Asp640 are supposed to be involved in the electrochemical proton gradient that provides energy to the transporter.[14] The last hydrophobic subpocket harbors the cyclooctyl ring which approaches a set of alkyl side chains including Ile248, Ile291, Ile292, and Val643.

Even though the considered MIC values are clearly influenced by lipophilicity as evidenced by Table 1 and as discussed above, docking results are in line with the reported activity values and allow in-depth rationalization of the obtained SARs. Thus, the above mentioned apolar residues surrounding the indole ring can easily explain the negative influence of polar substituents as seen in the amino derivatives (e.g., **6**) and indeed the computed complexes confirm that the amino group is never involved in clear polar contacts but at most bumps against Phe644. Again, the disfavored status of position 5 (see, for example, compound **8**) on the indole ring can be explained by considering that the substituent approaches the less flexible backbone atoms of Thr277 and Val288. Halogen substituents clearly make a positive contribution to binding due to their lipophilicity although the computed complexes do not show clear halogen bonds involving these substituents (see Figure 6B). The relevance of the H-bond involving the indole NH group is witnessed by the inactivity of the benzothiazole derivative (**42**).

The rich set of H-bonds stabilized by the amide moiety easily explains why even subtle modifications in that moiety have marked detrimental effects. Notably, the amide moiety determines the overall pose of the bound inhibitor, and indeed the computed complex for **40** shows a flipped pose in which the cycloheptyl ring takes the place of the indole moiety to allow the amide interactions to be properly elicited. Finally, the role of the *N*-linked moiety appears to be completely governed by its lipophilicity, a finding easily explainable when considering the above-mentioned set of surrounding apolar residues. Figure 6C shows the putative complex for **26** and reveals that the isopinocampheyl moiety is conveniently arranged within the apolar subpocket with all the methyl substituents suitably approaching alkyl side

chains, which also provides the basis for the observed stereoselectivity of these derivatives. The inactivity of the noncyclic derivatives (**28-31**) may have three explanations since (a) linear substituents are less able to contact the surrounding apolar residues, (b) their flexibility may play a disfavoring entropic role, and (c) they can bump against Phe635 which restricts this subpocket. By contrast, even extended cyclic moieties (as seen in the spiro compounds **37** and **38**) are able to maximize their hydrophobic contacts while remaining reasonably far from Phe365.

The performed MD simulations are unsuitable for exploring large protein conformational shifts induced by the bound inhibitors but can be conveniently utilized to analyze the relevance (and stability) of each monitored interaction. The dynamic profile of these interactions as assessed by their distance average and standard deviation (see Table S2 in SI) allows for some interesting considerations. All H-bonds show similar profiles which are suggestive of an overall marked stability of such interactions. Indeed, the distance profile of these H-bonds shows a roughly constant trend, apart from the contact involving Asp640 which reveals two distinct and alternating distance clusters around 2.7 Å and 4.5 Å, respectively. Notably, the best correlations (see Figure S1 in SI) are obtained by the frames where this contact assumes the larger distance values probably as such an overall arrangement allows a proper accommodation even of the bulkiest inhibitors. Finally, the standard deviation values, which can be seen as descriptors of the interaction stability, reveals that the charge transfer interaction and the hydrophobic contacts possess the highest stability, thus confirming the pivotal role of such interactions in stabilizing the simulated complexes.

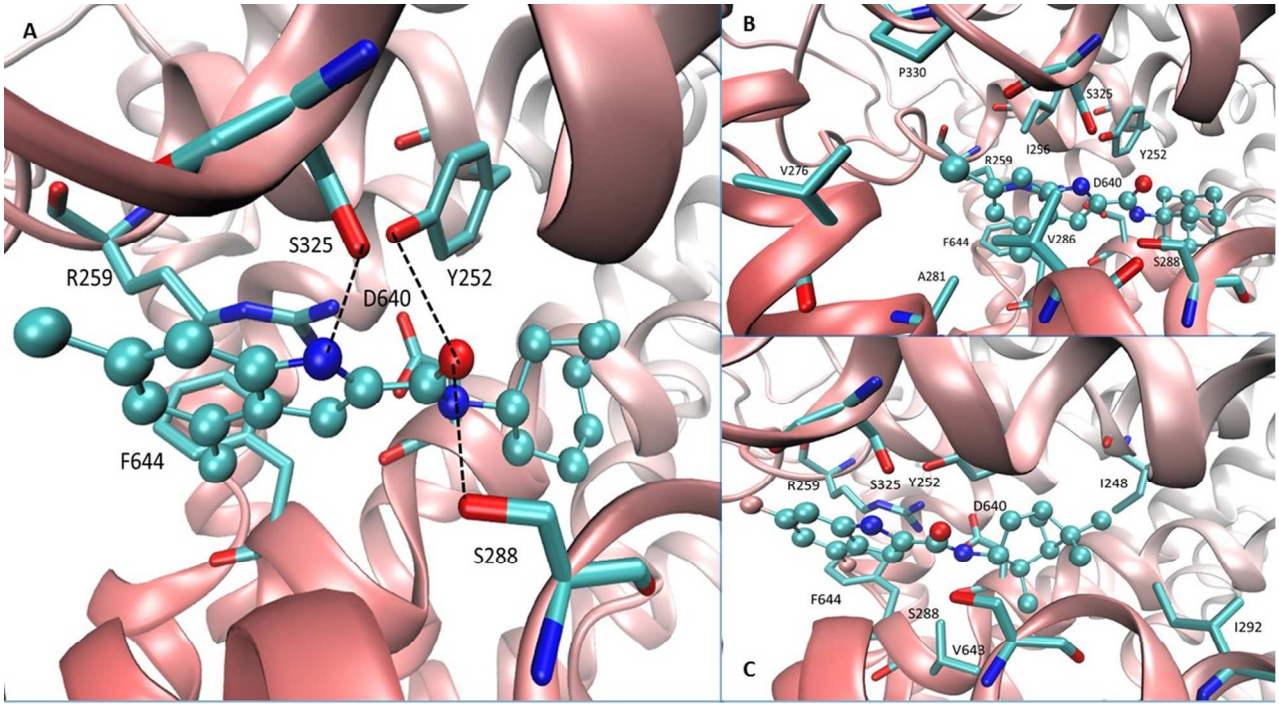

Figure 6. Main interactions stabilizing the putative MmpL3 complex with compound **3** (3A), **21** (3B), and **26** (3C).

The present work serves to underscore the importance of conducting a more comprehensive SAR program in order to identify the best candidate drug for advancement to clinical studies. We have assembled a total of over 80 indolecarboxamides to date, and we believe that the compound **26** identified in the present work represents a potential clinical candidate. As in our earlier work, it is likely that this compound acts as an inhibitor of the mycolic acid transporter MmpL3, although this activity may indirectly stem from its initial action on the proton motive force which leads in turn to inhibition of MmpL3. A putative homology model for the MmpL3 transporter has also been generated, and while this model can only be deemed approximate at this stage, it is useful in providing further possible insights into the SAR of the indolecarboxamides. In any event, compound **26** shows superior pharmaceutical properties, for by and large the compound displays acceptable ADMET parameters as well as *in vivo* activity. Additionally, the findings of synergy between **26** and rifampin are notable as this raises the possibility that

indolecarboxamide-containing treatment regimens with lower rifampin doses could be efficacious. Thus, in comparison to the Novartis compound **2** (NITD-304) that is under development by the TB Global Alliance, we believe that **26** may in fact represent a better candidate, as it is more effective in reducing the CFU count using the TB aerosol lung infection model.

Experimental Section

1. Chemistry

General information. The following carboxylic acids: 4-methyl-1*H*-indole-2-carboxylic acid, 5-methyl-1*H*-indole-2-carboxylic acid, 6-methyl-1*H*-indole-2-carboxylic acid, 7-methyl-1*H*-indole-2-carboxylic acid, 4,6-dichloro-1*H*-indole-2-carboxylic acid, and 6-bromo-1*H*-indole-2-carboxylic acid, were purchased from Sigma-Aldrich, Chem-Impex, Combi-blocks, and Ark Pharma. Anhydrous dichloromethane (CH_2Cl_2) was obtained by distillation over calcium hydride. ^{1}H NMR and ^{13}C NMR spectra were recorded on Bruker or JEOL spectrometers at 400 and 100 MHz, respectively. NMR spectra were reprocessed by ACDNMR Processor Academic Edition. Standard abbreviations indicating multiplicity were used as follows: s = singlet, d = doublet, dd = doublet of doublets, t = triplet, q = quadruplet, m = multiplet, and br = broad. HR-MS experiments were performed on Q-TOF-2TM (Micromass) and IT-TOF (Shimadzu) instruments. TLC was performed on Merck 60 F_{254} silica gel plates. Flash chromatography was performed using a CombiFlash® Rf system with RediSep® columns or manually using Merck silica gel (40–60 mesh). Final compounds were purified by preparative HPLC unless otherwise stated. Preparative HPLC employed an ACE 5-AQ (21.2 mm × 150 mm) column, with detection at 254 and 280 nm on a Shimadzu SCL-10A VP detector, flow rate = 17.0 mL/min. Method 1: 50–100% CH_3OH/H_2O in 30 min; 100% CH_3OH for 5 min; 100–50% CH_3OH/H_2O in 4 min.

Method 2: 25–100% CH_3OH/H_2O in 30 min; 100% CH_3OH for 5 min; 100–25% CH_3OH/H_2O in 4 min. Method 3: 15-100% CH_3OH/H_2O in 30 min; 100% CH_3OH for 5 min; 100–15% CH_3OH/H_2O in 4 min. Both solvents contained 0.05 vol % of trifluoroacetic acid (TFA). Purities of final compounds were established by analytical HPLC, which was carried out using an Agilent 1100 HPLC system with a Synergi 4 μm Hydro-RP 80A column, on a variable wavelength detector G1314A. Method 1: flow rate = 1.4 mL/min; gradient elution over 20 minutes, from 30% MeOH-H_2O to 100% MeOH with 0.05% TFA. Method 2: flow rate = 1.4 mL/min; gradient elution over 20 minutes, from 50% MeOH-H_2O to 70% MeOH with 0.05% TFA. The purity of all tested compounds was ≥95% as determined by the method described above (see supporting information).

General procedure for the synthesis of 4-42.

To a solution of the appropriate carboxylic acid (1 equiv) in anhydrous dichloromethane (CH_2Cl_2) (4 mL/mmol) at room temperature were added anhydrous hydroxybenzotriazole (HOBt, 1 equiv) and 1-ethyl-3-(3-dimethylaminopropyl)carbodiimide hydrochloride **(**EDC·HCl, 1 equiv) under an argon atmosphere. After stirring for 10 min, the appropriate substituted amine (1 equiv) and triethylamine (1.5 equiv) were added, and the reaction mixture was stirred at room temperature until disappearance of the starting material (usually 12 to 16 h). After this time water (2 mL) was added, and the mixture was extracted with EtOAc (3×10 mL). The organic layers were separated, washed with brine, dried over anhydrous Na_2SO_4, filtered, and concentrated under reduced pressure. The residue was purified by flash chromatography on SiO_2 using 0-40% EtOAc-Hexane gradient (unless specified differently) to obtain the indolecarboxamides in yields

ranging from 34 to 95%, which were further purified by preparative HPLC unless otherwise stated.

***N*-Cycloheptyl-4-methyl-1*H*-indole-2-carboxamide (4).** Yield 84% (white powder). ^{1}H NMR (400 MHz, d_6-DMSO) δ 11.5 (s, 1H), 8.24 (d, J = 8.0 Hz, 1H), 7.25 (d, J = 8.4 Hz, 1H), 7.22 (s, 1H), 7.05 (dd, J = 7.2, 8.0 Hz, 1H), 6.83 (d, J = 7.2 Hz, 1H), 4.01 (m, 1H), 2.48 (s, 3H), 1.91-1.87 (m, 2H), 1.71-1.54 (m, 10H); ^{13}C NMR (100 MHz, d_6-DMSO) δ 159.9, 136.1, 131.4, 130.2, 127.3, 123.2, 119.5, 109.8, 101.2, 49.9, 34.4 (2C), 27.9 (2C), 23.8 (2C), 18.5. HRMS (ESI) *m/z* calcd for $C_{17}H_{23}N_2O$ ($[M+H]^+$) 271.1805; found: 271.1808.

***N*-Cyclooctyl-4-methyl-1*H*-indole-2-carboxamide (5).** Yield 74% (white powder). ^{1}H NMR (400 MHz, d_6-DMSO) δ 11.5 (s, 1H), 8.22 (d, J = 8.0 Hz, 1H), 7.25 (d, J = 9.2 Hz, 1H), 7.22 (s, 1H), 7.05 (t, J = 7.6 Hz, 1H), 6.83 (d, J = 7.2 Hz, 1H), 4.05 (m, 1H), 2.49 (s, 3H), 1.82-1.67 (m, 6H), 1.61-1.52 (m, 8H); ^{13}C NMR (100 MHz, d_6-DMSO) δ 159.9, 136.1, 131.4, 130.2, 127.3, 123.2, 119.5, 109.8, 101.2, 48.9, 31.6 (2C), 26.9 (2C), 25.0, 23.4 (2C), 18.5. HRMS (ESI) *m/z* calcd for $C_{18}H_{25}N_2O$ ($[M+H]^+$) 285.1961; found: 285.1967.

4-Amino-*N*-cyclooctyl-1*H*-indole-2-carboxamide (6). Yield 78 % (white powder). ^{1}H NMR (400 MHz, CD_3OD) δ 7.45 (d, J = 8.4 Hz, 1H), 7.26 (m, 1H), 7.21 (s, 1H), 7.00 (d, J = 7.2 Hz, 1H), 4.18 (m, 1H), 1.94-1.64 (m, 14H); ^{13}C NMR (100 MHz, CD_3OD) δ 162.2, 139.4, 134.0, 125.4, 125.3, 122.3, 113.3, 112.4, 100.9, 51.4, 33.7 (2C), 28.3 (2C), 27.0, 25.3 (2C). HRMS (ESI) *m/z* calcd for $C_{17}H_{24}N_3O$ ($[M+H]^+$) 286.1914; found: 286.1918.

***N*-Cycloheptyl-5-methyl-1*H*-indole-2-carboxamide (7).** Yield 78% (off-white powder). ^{1}H NMR (400 MHz, d_6-DMSO) δ 11.4 (s, 1H), 8.18 (d, J = 7.6 Hz, 1H), 7.36 (s, 1H), 7.33 (d, J = 8.4 Hz, 1H), 7.07 (s, 1H), 7.00 (d, J = 8 Hz, 1H), 4.00 (m, 1H), 2.36 (s, 3H), 1.88 (m, 2H), 1.66-1.43 (m, 10H); ^{13}C NMR (100 MHz, d_6-DMSO) δ 159.9, 134.7, 132.0, 128.1, 127.3, 124.9,

120.6, 111.9, 102.0, 50.0, 34.4 (2C), 27.8 (2C), 23.9 (2C), 21.1. HRMS (ESI) *m/z* calcd for $C_{17}H_{23}N_2O$ ($[M+H]^+$) 271.1805; found: 271.1805.

***N*-Cyclooctyl-5-methyl-1*H*-indole-2-carboxamide (8).** Yield 74% (off-white powder). ^{1}H NMR (400 MHz, d_6-DMSO) δ 11.4 (s, 1H), 8.16 (d, J = 7.6 Hz, 1H), 7.36 (s, 1H), 7.32 (d, J = 8.4 Hz, 1H), 7.07 (s, 1H), 7.00 (d, J = 8.4 Hz, 1H), 4.04 (m, 1H), 2.36 (s, 3H), 1.81-1.68 (m, 6H), 1.60-1.53 (m, 8H); ^{13}C NMR (100 MHz, d_6-DMSO) δ 159.9, 134.7, 132.0, 128.1, 127.3, 124.9, 120.6, 111.9, 102.0, 48.9, 31.6 (2C), 26.9 (2C), 25.0, 23.5 (2C), 21.1. HRMS (ESI) *m/z* calcd for $C_{18}H_{25}N_2O$ ($[M+H]^+$) 285.1961; found: 285.1958.

5-Amino-*N*-cyclooctyl-1*H*-indole-2-carboxamide (9). Yield 71 % (white powder). ^{1}H NMR (400 MHz, d_6-DMSO) δ 11.79 (s, 1H), 9.85 (s, 2H), 8.31 (d, J = 8.0 Hz, 1H), 7.57 (s, 1H), 7.52 (d, J = 8.8 Hz, 1H), 7.22 (s, 1H), 7.14 (d, J = 8.4 Hz, 1H), 4.04 (m, 1H), 1.81-1.51 (m, 14H); ^{13}C NMR (100 MHz, d_6-DMSO) δ 159.4, 135.1, 133.9, 127.0, 118.0, 114.8, 133.4, 102.6, 49.0, 31.6 (2C), 26.9 (2C), 25.0, 23.4 (2C). HRMS (ESI) calcd for $C_{17}H_{24}N_3O$ ($[M+H]^+$) *m/z* 286.1914; found: 286.1912

***N*-Cyclooctyl-6-methyl-1*H*-indole-2-carboxamide (10).** Yield 78% (white powder). ^{1}H NMR (400 MHz, d_6-DMSO) δ 11.31 (s, 1H), 8.12 (d, J = 8.4 Hz, 1H), 7.47 (d, J = 8.4 Hz, 1H), 7.20 (s, 1H), 7.09 (s, 1H), 6.86 (d, J = 8.4 Hz, 1H), 4.03 (m, 1H), 2.38 (s, 3H), 1.77-1.51 (m, 14H); ^{13}C NMR (100 MHz, d_6-DMSO) δ 159.9, 136.7, 132.3, 131.5, 125.0, 121.6, 121.0, 111.7, 102.4, 48.8, 31.6 (2C), 26.9 (2C), 25.0, 23.4 (2C), 21.5. HRMS (ESI) calcd for $C_{18}H_{25}N_2O$ ($[M+H]^+$) *m/z* 285.1961; found: 285.1959.

6-Bromo-*N*-cyclooctyl-1*H*-indole-2-carboxamide (11). The title compound was obtained by following the general procedure. The crude material was purified by flash column chromatography on SiO_2 with a hexane-EtOAc gradient as the eluent followed by

recrystallization from ethyl acetate to give an off-white solid (155 mg, 44% on a 1.0 mmolar scale). ^{1}H NMR (d_6-DMSO) δ 11.61 (s, 1H), 8.26 (d, J = 7.8 Hz, 1H), 7.54 (d, J = 8.3 Hz, 1H), 7.53 (overlapping d, J = 1.1 Hz, 1H), 7.15 (s, 1H), 7.11 (dd, J = 8.5, 1.4 Hz, 1H), 1.75 – 1.40 (m, 15H); ^{13}C NMR (d_6-DMSO) δ 160.0, 137.6, 133.5, 126.6, 123.8, 123.1, 116.3, 115.2, 103.1, 49.5, 32.1 (2C), 27.4 (2C), 25.5, 24.0 (2C). HRMS (ESI) calcd for $C_{17}H_{22}BrN_2O$ ($[M + H]^+$) *m/z* 349.0915; found 349.0925.

***N*-(1-Adamantanyl)-6-bromo-1*H*-indole-2-carboxamide (12).** The title compound was obtained by following the general procedure. The crude material was purified by flash column chromatography on SiO_2 with a hexane -EtOAc gradient as the eluent followed by recrystallization from ethyl acetate to give an off-white solid (238 mg, 64% on a 1.0 mmolar scale). ^{1}H NMR (d_6-DMSO) δ 11.55 (s, 1H), 7.62 (s, 1H), 7.53 (s, 1H), 7.52 (overlapping d, J = 8.8 Hz, 1H), 7.15 (s, 1H), 7.10 (dd, J = 8.6, 1.6 Hz, 1H), 2.09 – 2.00 (m, 9H), 1.62 (br s, 6H); ^{13}C NMR (d_6-DMSO) δ 160.6, 137.5, 134.0, 126.6, 123.8, 123.1, 116.3, 115.1, 103.4, 52.2, 41.5 (3C), 36.6 (3C), 29.4 (3C). HRMS (ESI) *m/z* calcd for $C_{19}H_{22}BrN_2O$ ($[M + H]^+$) 373.0915; found 373.0918.

6-Bromo-*N*-((1*R*,2*R*,3*R*,5*S*)-2,6,6-trimethylbicyclo[3.1.1]heptan-3-yl)-1*H*-indole-2-carboxamide (13).

The title compound was obtained by following the general procedure. The crude material was purified by flash column chromatography on SiO_2 with a hexane-EtOAc gradient as the eluent followed by recrystallization from ethyl acetate to give a white solid (260 mg, 69% on a 1.0 mmolar scale). ^{1}H NMR (d_6-DMSO) δ 11.64 (s, 1H), 8.36 (d, J = 8.7 Hz, 1H), 7.55 (overlapping d, J = 8.7 Hz, 1H), 7.54 (s, 1H), 7.17 (d, J = 1.4 Hz, 1H), 7.12 (dd, J = 8.7, 1.8 Hz, 1H), 4.33 (m, 1H), 2.41 – 2.29 (m, 2H), 2.02 (quintuplet-d, J = 7.3, 0.9 Hz, 1H), 1.90 – 1.89 (m, 1H), 1.76 (t, J

= 5.3 Hz, 1H), 1.65 (ddd, *J* = 13.6, 6.5, 1.8 Hz, 1H), 1.18 (s, 3H), 1.17 (overlapping d, *J* = 12.3 Hz, 1H), 1.02 (s, 3H), 1.01 (overlapping d, *J* = 8.7 Hz, 3H); ^{13}C NMR (*d*$_6$-DMSO) δ 160.7, 137.6, 133.4, 126.6, 123.9, 123.1, 116.4, 115.2, 103.0, 47.8, 47.6, 44.4, 41.6, 38.9, 36.4, 34.3, 28.4, 23.8, 21.2. HRMS (ESI) calcd for $C_{19}H_{24}BrN_2O$ ($[M + H]^+$) *m/z* 375.1072; found 375.1053.

***N*-Cycloheptyl-7-methyl-1*H*-indole-2-carboxamide (14).** Yield 71% (white powder). ^{1}H NMR (400 MHz, *d*$_6$-DMSO) δ 11.2 (s, 1H), 8.20 (d, *J* = 8.0 Hz, 1H), 7.43 (d, *J* = 7.2 Hz, 1H), 7.14 (s, 1H), 6.98 (m, 2H), 4.00 (m, 1H), 2.51 (s, 3H), 1.93-1.88 (m, 2H), 1.71-1.42 (m, 10H); ^{13}C NMR (100 MHz, *d*$_6$-DMSO) δ 159.8, 136.0, 132.2, 126.7, 123.7, 121.6, 119.9, 118.8, 103.9, 50.0, 34.4 (2C), 27.9 (2C), 23.9 (2C), 17.1. HRMS (ESI) *m/z* calcd for $C_{17}H_{23}N_2O$ ($[M+H]^+$) 271.1805; found: 271.1803.

***N*-Cyclooctyl-7-methyl-1*H*-indole-2-carboxamide (15).** Yield 74% (white powder). ^{1}H NMR (400 MHz, *d*$_6$-DMSO) δ 11.2 (s, 1H), 8.18 (d, *J* = 8.0 Hz, 1H), 7.43 (d, *J* = 7.2 Hz, 1H), 7.14 (s, 1H), 6.96 (m, 2H), 4.06 (m, 1H), 2.51 (s, 3H), 1.83-1.67 (m, 6H), 1.62-1.50 (m, 8H); ^{13}C NMR (100 MHz, *d*$_6$-DMSO) δ 159.8, 136.0, 132.2, 126.7, 123.7, 121.6, 119.8, 118.8, 103.9, 48.9, 31.7 (2C), 26.9 (2C), 25.1, 23.5 (2C), 17.1. HRMS (ESI) calcd for $C_{18}H_{25}N_2O$ ($[M+H]^+$) *m/z* 285.1961; found: 285.1958.

***N*-Cycloheptyl-5,7-dimethyl-1*H*-indole-2-carboxamide (16).** Yield 80% (off-white powder). ^{1}H NMR (400 MHz, *d*$_6$-DMSO) δ 11.1 (s, 1H), 8.14 (d, *J* = 8.0 Hz, 1H), 7.18 (s, 1H), 7.03 (s, 1H), 6.80 (s, 1H), 3.99 (m, 1H), 2.46 (s, 3H), 2.32 (s, 3H), 1.92-1.87 (m, 2H), 1.70-1.53 (m, 10H); ^{13}C NMR (100 MHz, *d*$_6$-DMSO) δ 159.8, 134.5, 132.1, 128.3, 127.0, 125.6, 121.2, 118.1, 103.4, 50.0, 34.4 (2C), 27.9 (2C), 23.8 (2C), 21.0, 17.0. HRMS (ESI) *m/z* calcd for $C_{18}H_{25}N_2O$ ($[M+H]^+$) 285.1961; found: 285.1957.

***N*-Cyclooctyl-5,7-dimethyl-1H-indole-2-carboxamide (17).** Yield 82% (off-white powder). ^{1}H NMR (400 MHz, d_6-DMSO) δ 11.1 (s, 1H), 8.14 (d, J = 8.0 Hz, 1H), 7.19 (s, 1H), 7.04 (s, 1H), 6.80 (s, 1H), 4.05 (m, 1H), 2.47 (s, 3H), 2.32 (s, 3H), 1.82-1.62 (m, 6H), 1.58-1.52 (m, 8H); ^{13}C NMR (100 MHz, d_6-DMSO) δ 159.8, 134.5, 132.1, 128.3, 127.0, 125.6, 121.2, 118.1, 103.4, 48.9, 31.7 (2C), 26.9 (2C), 25.1, 23.5 (2C), 21.0, 17.0. HRMS (ESI) *m/z* calcd for $C_{19}H_{27}N_2O$ ($[M+H]^+$) 299.2118; found: 299.2118.

***N*-Cycloheptyl-4,6-dimethoxy-1*H*-indole-2-carboxamide (18).** Yield 87 % (white powder). ^{1}H NMR (400 MHz, d_6-DMSO) δ 11.3 (s, 1H), 8.06 (d, J = 8.0 Hz, 1H), 7.19 (s, 1H), 6.49 (s, 1H), 6.16 (s, 1H), 3.98 (m, 1H), 3.84 (s, 3H), 3.75 (s, 3H), 1.89-1.84 (m, 2H), 1.67-1.39 (m, 10H); ^{13}C NMR (100 MHz, d_6-DMSO) δ 159.9, 158.1, 153.9, 137.8, 129.4, 112.7, 100.5, 91.8, 86.9, 55.2, 55.1, 49.8, 34.4 (2C), 27.9 (2C), 23.8 (2C). HRMS (ESI) calcd for $C_{18}H_{25}N_2O_3$ ($[M+H]^+$) 317.1860; found: 317.1851.

***N*-Cyclooctyl-4,6-dimethoxy-1*H*-indole-2-carboxamide (19).** Yield 87 % (white powder). ^{1}H NMR (400 MHz, d_6-DMSO) δ 11.3 (s, 1H), 8.03 (d, J = 8.0 Hz, 1H), 7.18 (s, 1H), 6.48 (s, 1H), 6.16 (s, 1H), 3.99 (m, 1H), 3.84 (s, 3H), 3.75 (s, 3H), 1.79-1.50 (m, 14H); ^{13}C NMR (100 MHz, d_6-DMSO) δ 159.8, 158.1, 153.9, 137.8, 129.4, 112.7, 100.5, 91.7, 86.9, 55.2, 55.1, 48.7, 31.5 (2C), 26.9 (2C), 25.0, 23.4 (2C). HRMS (ESI) *m/z* calcd for $C_{19}H_{27}N_2O_3$ ($[M+H]^+$) 331.2016; found: 331.2001.

4,6-Dichloro-*N*-cyclooctyl-1*H*-indole-2-carboxamide (20). Yield 75 % (white powder). ^{1}H NMR (400 MHz, d_6-DMSO) δ 12.02 (s, 1H), 8.46 (d, J = 8.4 Hz, 1H), 7.41 (s, 1H), 7.33 (s, 1H), 7.21 (s, 1H), 4.03 (m, 1H), 1.81-1.50 (m, 14H); ^{13}C NMR (100 MHz, d_6-DMSO) δ 158.9, 136.7, 133.8, 127.5, 126.2, 124.8, 119.3, 111.0, 100.6, 49.1, 31.4 (2C), 26.9 (2C), 25.0, 23.4 (2C). HRMS (ESI) *m/z* calcd for $C_{17}H_{21}N_2OCl_2$ ($[M+H]^+$) 339.1025; found: 339.1013.

***N*-(1-Adamantanyl)-4,6-dichloro-1*H*-indole-2-carboxamide (21).** The title compound was obtained by following the general procedure. The crude material was purified by flash column chromatography on SiO_2 with a hexane-EtOAc gradient as the eluent followed by recrystallization from methanol to give an off-white solid (190 mg, 52% on a 1.0 mmolar scale). ^{1}H NMR (d_6-DMSO) δ 11.89 (s, 1H), 7.81 (s, 1H), 7.36 (s, 1H), 7.30 (s, 1H), 7.15 (s, 1H), 2.07 – 1.97 (m, 9H), 1.61 (br s, 6H); ^{13}C NMR (d_6-DMSO) δ 160.1, 137.1, 134.8, 128.0, 126.8, 125.4, 119.8, 111.5, 101.4, 52.4, 41.4 (3C), 36.5 (3C), 29.4 (3C). HRMS (ESI) *m/z* calcd for $C_{19}H_{21}Cl_2N_2O$ ($[M + H]^+$) 363.1031; found 363.1037.

***N*-(*exo*-Bicyclo[2.2.1]heptan-2-yl)-4,6-dichloro-1*H*-indole-2-carboxamide (22).** The title compound was obtained by following the general procedure. The crude material was purified by flash column chromatography on SiO_2 with a hexane-EtOAc gradient as the eluent followed by recrystallization from hexane to give a pale yellow solid (120 mg, 37% on a 1.0 mmolar scale). ^{1}H NMR (d_6-DMSO) δ 11.97 (s, 1H), 8.26 (d, J = 6.9 Hz, 1H), 7.37 (s, 1H), 7.33 (s, 1H), 7.17 (d, J = 1.4 Hz, 1H), 3.72 (m, 1H), 2.22 (br s, 1H), 2.15 (br s, 1H), 1.64 – 1.35 (m, 5H), 1.18 – 1.07 (m, 3H); ^{13}C NMR (d_6-DMSO) δ 160.1, 137.2, 134.1, 128.1, 126.8, 125.3, 119.8, 111.6, 101.4, 53.3, 42.5, 38.4, 35.7, 35.5, 28.6, 26.8. HRMS (ESI) *m/z* calcd for $C_{16}H_{17}Cl_2N_2O$ ($[M + H]^+$) 323.0718; found 323.0717.

4,6-Dichloro-*N*-(*endo*-(*1R*)-1,7,7-trimethylbicyclo[2.2.1]heptan-2-yl)-1*H*-indole-2-carboxamide (23). The title compound was obtained by following the general procedure. The crude material was purified by flash column chromatography on SiO_2 with a hexane-EtOAc gradient as the eluent followed by recrystallization from hexane to give an off-white solid (175 mg, 48% on a 1.0 mmolar scale). ^{1}H NMR (d_6-DMSO) δ 11.99 (s, 1H), 8.23 (d, J = 8.7 Hz, 1H), 7.42 (s, 1H), 7.37 (s, 1H), 7.18 (d, J = 1.4 Hz, 1H), 4.35 (m, 1H), 2.14 (tt, J = 12.2, 3.6 Hz, 1H),

1.77 – 1.61 (m, 3H), 1.38 (m, 1H), 1.21 (t, J = 12.1 Hz, 1H), 1.12 (dd, J = 12.8, 5.0 Hz, 1H), 0.92 (s, 3H), 0.81 (s, 3H), 0.72 (s, 3H); ^{13}C NMR (d_6-DMSO) δ 160.9, 137.2, 134.1, 128.1, 126.8, 125.3, 119.9, 111.6, 101.4, 54.0, 50.5, 48.5, 45.0, 35.0, 28.3, 28.2, 20.3, 19.1, 14.6. HRMS (ESI) *m/z* calcd for $C_{19}H_{23}Cl_2N_2O$ ($[M + H]^+$) 365.1187; found 365.1184.

4,6-Dichloro-*N*-((1*R*,2*R*,3*R*,5*S*)-2,6,6-trimethylbicyclo[3.1.1]heptan-3-yl)-1*H*-indole-2-carboxamide (24). The title compound was obtained by following the general procedure. The crude material was purified by flash column chromatography on SiO_2 with a hexane-EtOAc gradient as the eluent followed by recrystallization from hexane to give an off-white solid (5.11 g, 76% on a 18.4 mmolar scale). ^{1}H NMR (d_6-DMSO) δ 12.01 (s, 1H), 8.51 (d, J = 8.7 Hz, 1H), 7.38 (s, 1H), 7.30 (s, 1H), 7.18 (d, J = 1.4 Hz, 1H), 4.34 (m, 1H), 2.42 – 2.30 (m, 2H), 2.03 (quintuplet, J = 6.9 Hz, 1H), 1.90 (br s, 1H), 1.76 (t, J = 5.3 Hz, 1H), 1.66 (dd, J = 13.1, 5.7 Hz, 1H), 1.17 (s, 3H), 1.15 – 1.00 (m, 1H), 1.02 (s, 6H); ^{13}C NMR (d_6-DMSO) δ 160.1, 137.3, 134.3, 128.0, 126.8, 125.3, 119.9, 111.6, 101.1, 47.8, 47.6, 44.4, 41.6, 38.9, 36.3, 34.3, 28.4, 23.8, 21.2. HPLC: t_R 16.9 min, purity 98.4%. HRMS (ESI) *m/z* calcd for $C_{19}H_{23}Cl_2N_2O$ ($[M + H]^+$) 365.1187; found 365.1203.

4,6-Dichloro-*N*-((1*S*,2*S*,3*S*,5*R*)-2,6,6-trimethylbicyclo[3.1.1]heptan-3-yl)-1*H*-indole-2-carboxamide (25). Yield: 74% (white solid). ^{1}H NMR (400 MHz, d_6-DMSO) δ 12.05 (s, 1H), 8.56 (d, J = 8.4 Hz, 1H), 7.43 (s, 1H), 7.35 (s, 1H), 7.22 (s, 1H), 4.39 (m, 1H), 2.47 – 2.36 (m, 2H), 2.08 (t, J = 6.8 Hz, 1H), 1.94 (br s, 1H), 1.81 (m, 1H), 1.72 (dd, J = 12.8, 5.2 Hz, 1H), 1.23 (s, 3H), 1.22 – 1.20 (m, 1H), 1.07 (s, 6H); ^{13}C NMR (100 MHz, d_6-DMSO) δ 159.6, 136.7, 133.7, 127.5, 126.2, 124.8, 119.3, 111.1, 100.6, 47.3, 47.1, 43.9, 41.1, 38.3, 35.8, 33.8, 27.9, 23.3, 20.6. HRMS (ESI) *m/z* calcd for $C_{19}H_{23}Cl_2N_2O$ ($[M+H]^+$) 365.1187; found: 365.1166.

4,6-Difluoro-*N*-((1*R*,2*R*,3*R*,5*S*)-2,6,6-trimethylbicyclo[3.1.1]heptan-3-yl)-1*H*-indole-2-carboxamide (26). The title compound was obtained by following the general procedure. The crude material was purified by flash column chromatography on SiO_2 with a hexane-EtOAc gradient as the eluent followed by recrystallization from ethyl acetate to give white solid (5.03 g, 82% on a 18.4 mmolar scale). ^{1}H NMR (d_6-DMSO) δ 11.92 (s, 1H), 8.37 (d, J = 8.2 Hz, 1H), 7.27 (d, J = 1.4 Hz, 1H), 6.98 (dd, J = 9.6, 1.8 Hz, 1H), 6.84 (td, J = 10.4, 2.1 Hz, 1H), 4.32 (m, 1H), 2.42 – 2.30 (m, 2H), 2.02 (quintuplet-d, J = 7.2, 0.9 Hz, 1H), 1.90 – 1.89 (m, 1H), 1.76 (td, J = 5.8, 1.1 Hz, 1H), 1.65 (ddd, J = 13.6, 6.5, 1.8 Hz, 1H), 1.18 (s, 3H), 1.15 (d, J = 9.6 Hz, 1H), 1.02 (s, 3H), 1.01 (overlapping d, J = 7.8 Hz, 3H); ^{13}C NMR (d_6-DMSO) δ 160.2, 159.6 (dd, J = 238.2, 12.0 Hz), 156.2 (dd, J = 248.2, 15.3 Hz), 138.1 (t, J = 13.9 Hz), 135.5 (d, J = 2.9 Hz), 113.6 (d, J = 22.0 Hz), 98.7, 95.7 (dd, J = 29.7, 23.0 Hz), 95.1 (dd, J = 25.4, 4.3 Hz), 47.8, 47.5, 44.5, 41.6, 38.8, 36.4, 34.3, 28.4, 23.8, 21.2. HRMS (ESI) *m/z* calcd for $C_{19}H_{23}F_2N_2O$ ($[M + H]^+$) 333.1778; found 333.1764.

4,6-Difluoro-*N*-((1*S*,2*S*,3*S*,5*R*)-2,6,6-trimethylbicyclo[3.1.1]heptan-3-yl)-1*H*-indole-2-carboxamide (27). Yield: 72 % (white solid). ^{1}H NMR (400 MHz, d_6-DMSO) δ 11.95 (s, 1H), 8.40 (d, J = 8.8 Hz, 1H), 7.32 (s, 1H), 7.35 (dd, J = 9.6, 1.6 Hz, 1H), 6.87 (td, J = 10.4, 2.0 Hz, 1H), 4.37 (m, 1H), 2.46 – 2.33 (m, 2H), 2.06 (quintuplet-d, J = 7.2, 1.2 Hz, 1H), 1.94 – 1.93 (m, 1H), 1.80 (t, J = 5.2 Hz, 1H) 1.69 (ddd, J = 13.6, 6.4, 2.0 Hz, 1H), 1.22 (s, 3H), 1.21 (d, J = 9.6 Hz, 1H), 1.18 (m, 4H), 1.06 – 1.04 (m, 6H); ^{13}C NMR (100 MHz, d_6-DMSO) δ 160.2 (dd, J = 236.7, 12.2 Hz) 159.7, 157.0 (dd, J = 246.7, 15.3 Hz), 137.7 (t, J = 13.3 Hz), 133.0 (d, J = 3.3 Hz), 113.2 (d, J = 21.7 Hz), 98.2, 95.3 (dd, J = 29.6, 23.1 Hz), 94.7 (dd, J = 25.7, 4.4 Hz), 47.3, 47.0, 43.9, 41.1, 38.3, 35.9, 33.8, 27.9, 23.2, 20.6. HRMS (ESI) *m/z* calcd for $C_{19}H_{23}F_2N_2O$ ($[M+H]^+$) 333.1778; found: 333.1757.

4,6-Dichloro-*N*-heptyl-1*H*-indole-2-carboxamide (28). The title compound was obtained by following the general procedure. The crude material was purified by flash column chromatography on SiO_2 with a hexane-EtOAc gradient as the eluent followed by recrystallization from hexane to give an off-white solid (175 mg, 53% on a 1.0 mmolar scale). ^{1}H NMR (d_6-DMSO) δ 12.03 (s, 1H), 8.61 (t, J = 5.5 Hz, 1H), 7.37 (s, 1H), 7.20 (s, 1H), 7.18 (d, J = 1.4 Hz, 1H), 3.25 – 3.20 (m, 2H), 1.49 (apparent quintuplet, J = 6.6 Hz, 2H), 1.26 – 1.22 (m, 8H), 0.81 (t, J = 6.9 Hz, 3H); ^{13}C NMR (d_6-DMSO) δ 160.6, 137.2, 134.2, 128.1, 126.8, 125.3, 119.9, 111.6, 100.9, 39.4, 31.8, 29.6, 29.0, 26.9, 22.6, 14.5. HRMS (ESI) *m/z* calcd for $C_{16}H_{21}Cl_2N_2O$ ($[M + H]^+$) 327.1031; found 327.1032.

4,6-Dichloro-*N*-octyl-1*H*-indole-2-carboxamide (29). The title compound was obtained by following the general procedure. The crude material was purified by flash column chromatography on SiO_2 with a hexane-EtOAc gradient as the eluent followed by recrystallization from hexane to give an off-white solid (253 mg, 74% on a 1.0 mmolar scale). ^{1}H NMR (d_6-DMSO) δ 12.01 (s, 1H), 8.59 (t, J = 5.5 Hz, 1H), 7.37 (s, 1H), 7.20 (s, 1H), 7.18 (d, J = 1.8 Hz, 1H), 3.26 – 3.20 (m, 2H), 1.49 (quin, J = 6.5 Hz, 2H), 1.25 – 1.21 (m, 10H), 0.81 (t, J = 6.6 Hz, 3H); ^{13}C NMR (d_6-DMSO) δ 160.6, 137.2, 134.2, 128.1, 126.8, 125.4, 119.9, 111.6, 100.9, 39.4, 31.8, 29.6, 29.2 (2C), 27.0, 22.6, 14.5. HRMS (ESI) *m/z* calcd for $C_{17}H_{23}Cl_2N_2O$ ($[M + H]^+$) 341.1187; found 341.1205.

(*E*)-4,6-Dichloro-*N*-(3,7-dimethylocta-2,6-dien-1-yl)-1*H*-indole-2-carboxamide (30). The title compound was obtained by following the general procedure. The crude material was purified by flash column chromatography on SiO_2 with a hexane-EtOAc gradient as the eluent to give an off-white solid upon concentration (180 mg, 49% on a 1.0 mmolar scale). ^{1}H NMR (d_6-DMSO) δ 12.04 (br s, 1H), 8.72 (t, J = 5.5 Hz, 1 H), 7.36 (m, 1H), 7.22 (d, J = 0.9 Hz, 1 H), 7.18 (d, J =

1.6 Hz, 1 H), 5.20 (t, *J* = 6.2 Hz, 1 H), 5.04 (t, *J* = 6.9 Hz, 1 H), 3.85 (t, *J* = 6.2 Hz, 2 H), 2.05 – 1.99 (m, 2H), 1.96 – 1.92 (m, 2H), 1.65 (s, 3H), 1.58 (s, 3H), 1.51 (s, 3H); ^{13}C NMR (d_6-DMSO) δ 160.4, 137.8, 137.2, 134.1, 131.4, 128.1, 126.8, 125.4, 124.4, 121.5, 119.9, 111.6, 101.1, 39.5, 37.4, 26.5, 26.0, 18.1, 16.6. HRMS (ESI) *m/z* calcd for $C_{19}H_{23}Cl_2N_2O$ ($[M + H]^+$) 365.1187; found 365.1157.

(*E*)-*N*-(3,7-Dimethylocta-2,6-dien-1-yl)-4,6-difluoro-1*H*-indole-2-carboxamide (31). The title compound was obtained by following the general procedure. The crude material was purified by flash column chromatography on SiO_2 with a hexane-EtOAc gradient as the eluent to give white powder upon concentration (250 mg, 75% on a 1.0 mmolar scale). ^{1}H NMR (d_6-DMSO) δ 11.95 (br s, 1H), 8.60 (t, *J* = 5.5 Hz, 1 H), 7.18 (d, *J* = 1.4 Hz, 1 H), 6.97 (dd, *J* = 9.4, 1.6 Hz, 1 H), 6.82 (td, *J* = 10.3, 1.8 Hz, 1 H), 5.20 (t, *J* = 6.2 Hz, 1 H), 5.03 (t, *J* = 6.6 Hz, 1 H), 3.85 (t, *J* = 6.0 Hz, 2 H), 2.04 – 1.99 (m, 2H), 1.95 – 1.92 (m, 2H), 1.64 (s, 3H), 1.57 (s, 3H), 1.51 (s, 3H); ^{13}C NMR (d_6-DMSO) δ 160.5, 159.6 (dd, *J* = 238.2, 12.0 Hz), 156.2 (dd, *J* = 248.7, 15.8 Hz), 138.0 (t, *J* = 14.4 Hz), 137.7, 133.4 (d, *J* = 3.8 Hz), 131.4, 124.4, 121.7, 113.6 (d, *J* = 21.1 Hz), 98.6, 95.6 (dd, *J* = 29.7, 24.0 Hz), 95.1 (dd, *J* = 25.9, 4.8 Hz), 39.5, 37.3, 26.5, 26.0, 18.1, 16.6. HRMS (ESI) *m/z* calcd for $C_{19}H_{23}F_2N_2O$ ($[M + H]^+$) 333.1778; found 333.1758.

4,6-Dichloro-*N*-[((1*R*,2*R*,5*R*)-6,6-dimethylbicyclo[3.1.1]heptan-2-yl)methyl]-1*H*-indole-2-carboxamide (32). The title compound was obtained by following the general procedure. The crude material was purified by flash column chromatography on SiO_2 with a hexane-EtOAc gradient as the eluent followed by recrystallization from ethyl acetate to give an off-white solid (215 mg, 59% on a 1.0 mmolar scale). ^{1}H NMR (d_6-DMSO) δ 12.05 (s, 1H), 8.63 (t, *J* = 5.7 Hz, 1H), 7.36 (br s, 1H), 7.20 (br s, 1H), 7.18 (d, *J* = 1.8 Hz, 1H), 3.30 – 3.16 (m, 2H), 2.31 – 2.21 (m, 2H), 1.94 – 1.74 (m, 5H), 1.47 (m, 1H), 1.13 (s, 3H), 1.03 (s, 3H), 0.81 (d, *J* = 9.2 Hz, 1H);

^{13}C NMR (d_6-DMSO) δ 160.6, 137.2, 134.2, 128.1, 126.7, 125.3, 119.9, 111.6, 100.9, 44.7, 43.3, 41.3, 41.2, 38.8, 33.3, 28.3, 26.2, 23.4, 19.6. HRMS (ESI) *m/z* calcd for $C_{19}H_{23}Cl_2N_2O$ ([M + H]$^+$) 365.1187; found 365.1164.

(*R*)-*N*-(1-Cyclohexylethyl)-4,6-dichloro-1*H*-indole-2-carboxamide (33). The title compound was obtained by following the general procedure. The crude material was purified by flash column chromatography on SiO_2 with a hexane-EtOAc gradient as the eluent to give a pale brown solid upon concentration (157 mg, 46% on a 1.0 mmolar scale). ^{1}H NMR (d_6-DMSO) δ 12.00 (s, 1H), 8.31 (d, J = 8.7 Hz, 1H), 7.36 (m, 1H), 7.29 (d, J = 1.4 Hz, 1H), 7.17 (d, J = 1.8 Hz, 1H), 3.81 (m, 1H), 1.73 – 1.65 (m, 4H), 1.56 (m, 1H), 1.36 (m, 1H), 1.16 – 1.04 (m, 6H), 0.96 – 0.88 (m, 2H); ^{13}C NMR (d_6-DMSO) δ 160.0, 137.2, 134.3, 128.0, 126.8, 125.3, 119.8, 111.6, 101.0, 49.6, 43.0, 29.7, 29.5, 26.5, 26.2 (2C), 18.2. HRMS (ESI) *m/z* calcd for $C_{17}H_{21}Cl_2N_2O$ ([M + H]$^+$) 339.1031; found 339.1011.

(*R*)-*N*-(1-Cyclohexylethyl)-4,6-difluoro-1*H*-indole-2-carboxamide (34). The title compound was obtained by following the general procedure. The crude material was purified by flash column chromatography on SiO_2 with a hexane-EtOAc gradient as the eluent to give a pale yellow solid upon concentration (260 mg, 65% on a 1.0 mmolar scale). ^{1}H NMR (d_6-DMSO) δ 11.90 (s, 1H), 8.15 (d, J = 8.7 Hz, 1H), 7.25 (d, J = 1.4 Hz, 1H), 6.96 (dd, J = 9.1, 0.9 Hz, 1H), 6.83 (td, J = 10.3, 1.8 Hz, 1H), 3.80 (m, 1H), 1.72 – 1.54 (m, 5H), 1.35 (m, 1H), 1.18 – 1.04 (m, 6H), 0.95 – 0.89 (m, 2H); ^{13}C NMR (d_6-DMSO) δ 160.1, 159.6 (dd, J = 238.2, 12.0 Hz), 156.2 (dd, J = 248.2, 16.3 Hz), 138.0 (t, J = 14.4 Hz), 135.5 (d, J = 1.9 Hz), 113.6 (d, J = 22.0 Hz), 98.6, 95.6 (dd, J = 29.7, 23.0 Hz), 95.1 (dd, J = 25.9, 3.8 Hz), 49.5, 43.0, 29.7, 29.4, 26.5, 26.2 (2C), 18.2. HRMS (ESI) *m/z* calcd for $C_{17}H_{21}F_2N_2O$ ([M + H]$^+$) 307.1622; found 307.1609.

4,6-Dichloro-*N*-(2,3-dihydro-1*H*-inden-2-yl)-1*H*-indole-2-carboxamide (35). The title compound was obtained by following the general procedure. The crude material was purified by flash column chromatography on SiO_2 with a hexane-EtOAc gradient as the eluent to give a grey solid upon concentration (223 mg, 65% on a 1.0 mmolar scale). ^{1}H NMR (d_6-DMSO) δ 12.05 (br s, 1H), 8.85 (d, J = 6.9 Hz, 1H), 7.37 (br s, 1H), 7.28 (br s, 1H), 7.21 (dd, J = 5.3, 3.4 Hz, 2H), 7.18 (d, J = 1.8 Hz, 1H), 7.12 (d, J = 3.6 Hz, 2H), 4.67 (quintuplet, J = 6.8 Hz, 1H), 3.23 (dd, J = 16.0, 7.8 Hz, 2H), 2.92 (dd, J = 15.8, 6.2 Hz, 2H); ^{13}C NMR (d_6-DMSO) δ 160.6, 141.7 (2C), 137.3, 133.9, 128.2, 127.0 (2C), 126.8, 125.3, 125.0 (2C), 119.9, 111.6, 101.5, 50.9, 39.5 (2C). HRMS (ESI) *m/z* calcd for $C_{18}H_{15}Cl_2N_2O$ ($[M + H]^+$) 345.0561; found 345.0552.

***N*-4,6-Difluoro-(2,3-dihydro-1*H*-inden-2-yl)- 1*H*-indole-2-carboxamide (36).** The title compound was obtained by following the general procedure. The crude material was purified by flash column chromatography on SiO_2 with a hexane-EtOAc gradient as the eluent to give a white powder upon concentration (204 mg, 65% on a 1.0 mmolar scale). ^{1}H NMR (d_6-DMSO) δ 11.97 (s, 1H), 8.70 (d, J = 6.9 Hz, 1H), 7.25 (br s, 1H), 7.22 – 7.19 (m, 2H), 7.14 – 7.10 (m, 2H), 6.98 (dd, J = 9.4, 1.6 Hz, 1H), 6.83 (td, J = 10.4, 2.1 Hz, 1H), 4.66 (m, 1H), 3.23 (dd, J = 16.0, 7.8 Hz, 2H), 2.92 (dd, J = 16.0, 6.0 Hz, 2H); ^{13}C NMR (d_6-DMSO) δ 160.7, 159.6 (dd, J = 238.6, 12.5 Hz), 156.2 (dd, J = 248.2, 15.3 Hz), 141.7 (2C), 138.1 (t, J = 14.4 Hz), 133.2 (d, J = 2.9 Hz), 127.0 (2C), 125.0 (2C), 113.6 (d, J = 21.1 Hz), 99.0, 95.6 (dd, J = 29.7, 23.0 Hz), 95.1 (dd, J = 25.9, 3.8 Hz), 50.8, 39.5 (2C). HRMS (ESI) *m/z* calcd for $C_{18}H_{15}F_2N_2O$ ($[M + H]^+$) 313.1152; found 313.1132.

4,6-Dichloro-*N*-(spiro[5.5]undecan-3-yl)-1*H*-indole-2-carboxamide (37). The title compound was obtained by following the general procedure. The crude material was purified by flash column chromatography on SiO_2 with a hexane-EtOAc gradient as the eluent to give a yellow

powder upon concentration (151 mg, 65% on a 0.61 mmolar scale). ^{1}H NMR (d_6-DMSO) δ 12.01 (s, 1H), 8.38 (d, J = 6.2 Hz, 1H), 7.36 (dd, J = 1.8, 0.9 Hz, 1H), 7.24 (d, J = 1.4 Hz, 1H), 7.17 (d, J = 1.4 Hz, 1H), 3.71 (m, 1H), 1.63 – 1.56 (m, 4H), 1.51 – 1.44 (m, 2H), 1.42 – 1.34 (m, 8H), 1.16 – 1.14 (m, 2H), 1.10 – 1.03 (m, 2H); ^{13}C NMR (d_6-DMSO) δ 159.7, 137.2, 134.3, 128.0, 126.8, 125.3, 119.9, 111.6, 101.0, 49.0, 41.0, 35.4 (2C), 32.1, 31.8, 27.7 (2C), 27.0, 21.9, 21.6. HRMS (ESI) *m/z* calcd for $C_{20}H_{25}Cl_2N_2O$ ($[M + H]^+$) 379.1344; found 379.1316.

4,6-Difluoro-*N*-(spiro[5.5]undecan-3-yl)-1*H*-indole-2-carboxamide (38). The title compound was obtained by following the general procedure. The crude material was purified by flash column chromatography on SiO_2 with a hexane-EtOAc gradient as the eluent to give an off-white powder upon concentration (174 mg, 82% on a 0.61 mmolar scale). ^{1}H NMR (d_6-DMSO) δ 11.92 (br s, 1H), 8.24 (d, J = 8.2 Hz, 1H), 7.20 (s, 1H), 6.96 (dd, J = 9.2, 1.4 Hz, 1H), 6.83 (td, J = 10.4, 2.1 Hz, 1H), 3.70 (m, 1H), 1.63 – 1.57 (m, 4H), 1.50 – 1.35 (m, 10H), 1.17 – 1.15 (m, 2H), 1.13 – 1.04 (m, 2H); ^{13}C NMR (d_6-DMSO) δ 159.8, 159.6 (dd, J = 238.2, 12.0 Hz), 156.2 (dd, J = 248.2, 15.3 Hz), 138.0 (t, J = 13.9 Hz), 133.5 (d, J = 2.9 Hz), 113.6 (d, J = 22.0 Hz), 98.6, 95.6 (dd, J = 29.7, 23.9 Hz), 95.1 (dd, J = 25.9, 3.8 Hz), 48.9, 41.0, 35.4 (2C), 32.1, 31.9, 27.7 (2C), 27.0, 21.9, 21.6. HRMS (ESI) *m/z* calcd for $C_{20}H_{25}F_2N_2O$ ($[M + H]^+$) 347.1935; found 347.1914.

4,6-Dichloro-*N*-(9-methyl-9-azabicyclo[3.3.1]nonan-3-yl)-1*H*-indole-2-carboxamide (39). Yield: 81 % (white solid). ^{1}H NMR (400 MHz, d_6-DMSO) δ 12.2 (s, 1H), 8.65 (d, J = 8.0 Hz, 1H), 7.43 (s, 1H), 7.26 (s, 1H), 7.22 (d, J = 1.6 Hz, 1H), 4.60 (m, 1H), 3.67 (d, J = 8.0 Hz, 2H), 2.83 (s, 3H), 2.41 (m, 2H), 2.05 (m, 3H), 1.79 (t, J = 11.6 Hz, 2H), 1.58 – 1.43 (m, 3H); ^{13}C NMR (100 MHz, d_6-DMSO) δ 159.7, 158.5, 158.2, 136.9, 133.2, 127.9, 126.4, 124.8, 119.6,

111.2, 100.9, 52.5, 37.8, 37.3, 30.8, 22.8, 11.4. HRMS (ESI) *m/z* calcd for $C_{18}H_{22}Cl_2N_3O$ ($[M+H]^+$) 366.1108; found: 366.1140.

Ethyl (*E*)-2-[(3,5-Dimethoxyphenyl)amino]-3-(dimethylamino)acrylate (55).

A solution of the aniline **54** (3.00 g, 19.6 mmol) and K_2CO_3 (4.06 g, 29.4 mmol) in acetone (40 mL) was heated at 60 °C for 1 h. Ethyl bromoacetate (2.60 mL, 23.5 mmol) was added slowly, and the resulting mixture was heated at 60 °C overnight. The mixture was cooled, filtered, and concentrated *in vacuo*. The obtained crude product was purified by flash column (SiO_2) chromatography (hexane/EtOAc; gradient) to obtain ethyl (3,5-dimethoxyphenyl)glycinate (2.95 g, 63%). ^{1}H NMR ($CDCl_3$) δ 5.91 (m, 1H), 5.79 (d, J = 2.0 Hz, 1H), 4.24 (q, J = 7.2 Hz, 2H), 3.86 (s, 2H), 3.74 (s, 6H), 1.29 (t, J = 7.2 Hz, 3H); ^{13}C NMR ($CDCl_3$) δ 171.1, 161.9, 149.1, 92.0, 90.6, 61.5, 55.3, 45.9, 14.3.

Ethyl (3,5-dimethoxyphenyl)glycinate (2.95 g, 12.3 mmol) and dimethylformamide dimethyl acetal (2.45 mL, 18.5 mmol) were placed in a 20 mL microwave vessel with a stir bar. The mixture was irradiated for 10 min at 150 °C. The resulting yellowish-orange solution was concentrated *in vacuo*, dried in an oil vacuum pump, and purified by flash column (SiO_2) chromatography (hexane/EtOAc; gradient) to obtain compound **55** (1.21 g, 33%). ^{1}H NMR ($CDCl_3$) δ 7.34 (s, 1H), 5.89 (m, 1H), 5.83 (d, J = 2.0 Hz, 1H), 4.10 (q, J = 7.2 Hz, 2H), 3.72 (s, 6H), 3.02 (s, 6H), 1.19 (t, J = 7.2 Hz, 2H); ^{13}C NMR ($CDCl_3$) δ 169.2, 161.8, 151.7, 146.2, 99.2, 92.7, 90.6, 59.9, 55.3, 42.0, 14.8.

4,6-Dimethoxy-1*H*-indole-2-carboxylic acid (56).

Compound **55** (1.2 g, 4.1 mmol) was dissolved in CH_2Cl_2 (50 mL). $AlCl_3$ (0.54 g, 4.1 mmol) was added, and the reaction mixture was stirred for 24 - 48 h. The resulting solution was washed with

water and brine. The organic solution was dried over anhydrous Na_2SO_4 and concentrated, and the residue was purified by flash column (SiO_2) chromatography (hexane/EtOAc; gradient) to obtain the intermediate indolecarboxylate (0.83 g, 81%). A mixture of the indolecarboxylate (0.83 g, 3.33 mmol) and LiOH (0.40 g, 16.6 mol) in EtOH (10 mL) was refluxed with TLC monitoring until no starting material was observed. After completion, the mixture was concentrated, and H_2O (10 mL) was added to dissolve the solid. The resulting solution was acidified to a pH >3 with 6N HCl solution, and the precipitate was filtered and dried to obtain the carboxylic acid **56** as a tan solid (0.67 g, 91%). ^{1}H NMR (d_6-DMSO) δ 12.63 (s, 1H), 11.57 (s, 1H), 6.96 (m, 1H), 6.46 (s, 1H), 6.18 (m, 1H), 3.84 (s, 3H), 3.76 (s, 3H); ^{13}C NMR (d_6-DMSO) δ 162.5, 159.1, 154.1, 138.9, 125.7, 112.8, 105.1, 92.2, 86.7, 55.2, 55.1.

4,6-Dimethyl-1*H*-indole-2-carboxamide (57).

To a solution of the carboxylic acid **43** (0.30 g, 1.6 mmol) in anhydrous CH_2Cl_2 (5 mL) at room temperature were added anhydrous hydroxybenzotriazole (0.26 g, 1.9 mmol) and 1-ethyl-3-(3-dimethylaminopropyl)carbodiimide hydrochloride (0.36 g, 1.9 mmol) under an argon atmosphere. After stirring for 10 min, ammonium chloride (0.127 g, 2.38 mmol) and triethylamine (0.33 mL, 2.4 mmol) were added, and the reaction mixture was stirred at room temperature until disappearance of the starting material (usually 12 to 16 h). After this time water (2 mL) was added, and the mixture was extracted with EtOAc (3×10 mL). The organic layers were separated, washed with brine, dried over anhydrous Na_2SO_4, filtered, and concentrated under reduced pressure. The residue was purified by flash column (SiO_2) chromatography (0-10% CH_3OH/CH_2Cl_2) to obtain the indolecarboxamide **57** (0.29 g, 96 %). ^{1}H NMR (d_6-DMSO) δ 11.33 (s, indole NH), 7.86 (s, NH), 7.24 (s, NH), 7.11 (m, 1H), 7.02 (s, 1H), 6.66 (s, 1H), 2.43

(s, 3H), 2.34 (s, 3H); ^{13}C NMR (d_6-DMSO) δ 163.0, 136.7, 132.6, 130.5, 129.9, 125.3, 121.6, 109.4, 101.8, 21.5, 18.4.

***N*-[(4,6-Dimethyl-1*H*-indol-2-yl)methyl]cycloheptanecarboxamide (40).** To a cooled solution of compound **57** (0.29 g, 1.5 mmol) in 15 mL THF was added $LiAlH_4$ (6 equiv, 0.35g, 9.2 mmol) over 5 min. The ice bath was removed and the resulting solution heated to reflux under argon for 18 h. The mixture was cooled and the reagent quenched with aqueous Na_2SO_4 solution. The resulting precipitate was filtered off, the filtrate was concentrated, and the residue was purified by flash column (SiO_2) chromatography (0-10% CH_3OH/CH_2Cl_2) to obtain (4,6-dimethyl-1*H*-indol-2-yl)methylamine (0.14 g, 54 %). ^{1}H NMR ($CDCl_3$) δ 8.98 (s, 1H), 6.98 (s, 1H), 6.85 (s, 1H), 6.36 (s, 1H), 3.98 (s, 2H), 2.59 (s, 3H), 2.51 (s, 3H), 2.05 (s, 2H); ^{13}C NMR ($CDCl_3$) δ 138.6, 136.4, 131.4, 129.3, 126.1, 121.7, 108.5, 97.7, 39.6, 21.7, 18.8.

To a solution of the cycloheptanecarboxylic acid (0.13 g, 0.89 mmol) in anhydrous CH_2Cl_2 (5 mL) at room temperature were added anhydrous hydroxybenzotriazole (0.13 g, 0.97 mmol) and 1-ethyl-3-(3-dimethylaminopropyl)carbodiimide hydrochloride (0.19 g, 0.97 mmol) under an argon atmosphere. After stirring for 10 min, (4,6-dimethyl-1*H*-indol-2-yl)methylamine (0.14 g, 0.80 mmol) and triethylamine (0.17 mL, 1.2 mmol) were added, and the reaction mixture was stirred at room temperature until disappearance of the starting material (usually 12 to 16 h). After this time water (2 mL) was added, and the mixture was extracted with EtOAc (3×10 mL). The organic layers were separated, washed with brine, dried over anhydrous Na_2SO_4, filtered, and concentrated under reduced pressure. The crude product was initially purified by flash column (SiO_2) chromatography eluting with 0 - 10% CH_3OH/CH_2Cl_2 and further purified by preparative HPLC to obtain compound **40** as a white powder (0.16 g, 67 %). ^{1}H NMR (d_6-DMSO) δ 10.65 (s, 1H), 8.12 (s, 1H), 6.93 (s, 1H), 6.58 (s, 1H), 6.17 (s, 1H), 4.34 (s, 2H), 2.37-2.32 (m, 7H),

1.75-1.42 (m, 12H); ^{13}C NMR (d_6-DMSO) δ 176.2, 136.2, 135.9, 129.5, 127.8, 125.6, 120.7, 108.6, 97.4, 45.4, 36.1, 31.1 (2C), 27.9 (2C), 26.1 (2C), 21.4, 18.5. HRMS (ESI) *m/z* calcd for $C_{19}H_{27}N_2O$ ($[M+H]^+$) 299.2118; found: 299.2118.

***N*-[(4,6-Dimethyl-1*H*-indol-2-yl)methyl]cyclooctylamine (41).** To a cooled solution of compound **3** (0.39 g, 0.98 mmol) in THF (15 mL) was added $LiAlH_4$ (6 equiv, 0.22 g, 5.9 mmol) over 5 min. The ice bath was removed and the resulting solution heated to reflux under argon for 18 h. The mixture was cooled and the reagent quenched with aqueous Na_2SO_4 solution. The resulting precipitate was filtered off, the filtrate was concentrated, and the residue was purified by flash column (SiO_2) chromatography eluting with 0-10% CH_3OH/CH_2Cl_2. The crude product was further purified by prep HPLC to obtain compound **41** as a white powder (85% yield). ^{1}H NMR (400 MHz, d_6-DMSO) δ 11.1 (s, 1H), 8.89 (s, 1H), 7.02 (s, 1H), 6.66 (s, 1H), 6.55 (s, 1H), 4.31 (s, 2H), 3.25 (m, 1H), 2.41 (s, 3H), 2.35 (s, 3H), 1.99 (m, 2H), 1.70-1.38 (m, 14H); ^{13}C NMR (100 MHz, d_6-DMSO) δ 136.4, 131.1, 128.6, 128.1, 125.4, 121.4, 108.8, 101.7, 57.2, 41.0, 28.5 (2C), 25.9 (2C), 25.1, 23.2 (2C), 21.3, 18.4. HRMS (ESI) *m/z* calcd for $C_{19}H_{29}N_2$ ($[M+H]^+$) 285.2325; found: 285.2316.

***N*-[6-(Trifluoromethoxy)benzothiazol-2-yl]cycloheptanecarboxamide (42).** Yield 73% (white powder). ^{1}H NMR (400 MHz, d_6-DMSO) δ 12.38 (s, 1H), 8.10 (s, 1H), 7.81 (d, J = 8.0 Hz, 1H), 7.41 (d, J = 8.0 Hz, 1H), 2.73 (m, 1H), 1.88 (m, 2H), 1.69-1.52 (m, 10H); ^{13}C NMR (100 MHz, d_6-DMSO) δ 176.3, 159.6, 147.6, 143.9, 132.7, 121.3, 119.7, 114.9, 44.9, 30.5 (2C), 27.9 (2C), 25.9 (2C). HRMS (ESI) *m/z* calcd for $C_{16}H_{17}N_2O_2F_3S$ ($[M-H]^-$) 357.0890; found: 357.0906.

2. Biological Methods

Minimum inhibitory concentration (MIC). *M. tuberculosis* H37Rv was cultured to mid-log phase in 7H9 broth complemented with 10% OADC, 0.05% Tween 80, and 0.1% cholesterol. MIC determination was done as reported previously.[16, 28]

Pharmacokinetic study in mice. Female BALB/c mice (20 g each, Charles River Laboratories) were given a single dose of compound **26** and **2** at 100 mg/kg by oral gavage in a volume of 0.2 mL. At 0, 0.25, 0.5, 1, 2, 4, 8, and 24 h after compound administration, animals (n=3 per time point) were euthanized, and cardiac blood (~0.7 mL) was collected. Mouse lungs were removed, weighed, and stored at -80 °C. Plasma was separated by centrifugation at 12,000×*g* for 20 min at 4 °C and stored at -80 °C. For analysis, the lungs were homogenized by bead-beating in 0.5 mL of liquid chromatography/mass spectrometry (LC/MS) grade water, and supernatants were recovered by centrifugation at 12,000×g at 4 °C for 20 min. Concentrations of compound **26** and **2** in plasma and lung homogenate supernatants were analyzed with LC-tandem MS (LC-MS/MS, AB SCIEX QTRAP 5500 system) with the 4,6-dimethylindole-2-carboxamide analog (compound **2** in Lun et al., 2013) as internal standard. MS detection of mass transitions 81.0/333.1 and 154.1/333.1 for compound **26** and 186.0/339.1 and 151.0/339.1 for compound **2** was carried out. Concentration calculation was carried out using MultiQuant Software (Version 2.1, AB SCIEX). The pharmacokinetic profiles of the test compounds were analyzed from plasma and lung concentration-time data. Analyses of PK parameters were performed using noncompartmental modeling (WinNonlin PK software package, Version 6.4.0).

Serum inhibition titration (SIT). To test oral bioavailability in a biological-function assay, 6-week-old female BALB/c mice (20 g each) were used. Compounds **20**, **24**, and **26** were ground into homogenous suspensions in water containing 0.5% carboxymethylcellulose (CMC). A

single dose at 100 mg/kg was delivered orally. At 30, 60, and 120 minutes after administration, the mice were sacrificed,cardiac blood was collected, and serum samples were obtained. Isoniazid at 10 mg/kg was used as positive control. The vehicle (0.5% CMC) was used as negative control. Samples from 3 mice were pooled for each time point. The serum samples were 2-fold serially diluted in a 96-well microplate format and 10^4 CFU of *M. tuberculosis* H37Rv in 100 μL was added to each well. After incubation for 7 days at 37 °C, 32.5 μL of alamarBlue working reagent (1 part of 10% alamarBlue and 0.625 parts of 20% Tween 80) was added to each well, and the plates were further incubated for 16-18 hours and then read at Ex544nm/Em590nm. Relative fluorescence units were plotted against the serum titration.

Mouse infection and monotherapy model. Four-to-six-week-old female BALB/c mice were aerosol-infected with *M. tuberculosis* H37Rv using an inhalation system (Glas-Col Inc., Terre Haute, IN). At day 1, 5 mice were sacrificed for enumeration for CFU implantation in the lungs. From day 1 after infection, group of five mice were treated with 12.5, 25, 50, or 100 mg/kg of compound **26** or **2** by daily oral gavage (5 days per week). Ethambutol at 100 mg/kg was administered as positive control. Infected but untreated mice were used as negative control. At day 14 and 28 after treatment initiation, 5 mice from each treatment were sacrificed and the lungs removed. The lungs were ground to a homogenate, diluted, and plated on 7H11 selective agar plates, and CFUs per lung were determined.

***In vitro* synergy Bliss modeling.** Checkerboard design was carried out for an *in vitro* synergy study between **26** and rifampin. Two-fold serial dilution ranging from 4.0 to 0.0313 times the MIC for either compound was combined as shown in Table 1 in a 96-well microplate format. 1×10^4 CFUs of wild type *M. tuberculosis* H37Rv were added into each well to total volume of 200 μL. Controls consisting of the compound alone (**26** and rifampin) employing the same

dilutions were included. Also included were a blank control and full growth control. The alamarBlue assay was conducted as reported previously.[16, 28] Percentage inhibition was calculated. Bliss independence modeling[29] was applied to all wells with compound concentration below 1×MIC. Observed effect (f_{axyO}) and predicted effect (f_{axyP}) were calculated. Synergy (Δf_{axy} >0), Bliss independence (Δf_{axy} =0), or antagonism (Δf_{axy} <0) was assessed according to a previous report.[29]

***In vivo* synergy Bliss modeling.** Four-to-six-week-old female BALB/c mice were aerosol-infected with *M. tuberculosis* H37Rv as described above to achieve a day 1 implantation of 3.4-log CFU per lung. At day 14, four mice were sacrificed for CFU enumeration. From day 14 after infection, groups of four mice were treated with 100 mg/kg of compound **26** and rifampin at 10 mg/kg by oral gavage, separately with at least 1 h apart. Treatment was daily, 5 days per week. Compound **26** at 100 mg/kg alone and rifampin at 10 mg/kg alone were the control arms. Infected but untreated mice were negative control. At day 28 after treatment initiation, four mice from each treatment were sacrificed, and CFUs in the lungs were determined as above. Synergy between compound **26** and rifampicin was analyzed, and Bliss Modeling was applied.[29]

The Institutional Animal Care and Use Committee of the Johns Hopkins University School of Medicine approved all animal procedures in this study with the approved protocol number as MO13M156.

Acknowledgment

A.P.K. and W.B. acknowledge initial financial support for this project from the Howard Hughes Medical Institute. J.S. acknowledges Chicago State University College of Pharmacy and Chicago State University Center for Teaching and Research Excellence (Faculty Seed Grant) for generous financial support. The unlimited access to the NMR facility (JEOL 400) in the Department of Chemistry, Physics, and Engineering Studies at Chicago State University is acknowledged. A Faculty Development Stipend (J.S.) from Marshall B. Ketchum University College of Pharmacy is acknowledged.

Additional Information

[#] These authors contributed equally to this work

* Authors for correspondence: Alan P. Kozikowski: Phone: +1-312-996-7577; Fax: +1-312-996-7107; E-mail: kozikowa@uic.edu; William R. Bishai: Phone: +1-410-955-3507; E-mail: wbishai1@jhmi.edu

Supporting Information

Purity of the tested compounds and details on molecular model generation, optimization, and docking simulations

References

1. World Health Organization Global Tuberculosis Report 2015. *http://www.who.int/tb/publications/global_report/en/*, Accessed November 11, 2015.

2. *http://www.tballiance.org/why/economic-impact.php*, Accessed November 11, 2015.

3. Koul, A.; Arnoult, E.; Lounis, N.; Guillemont, J.; Andries, K., The challenge of new drug discovery for tuberculosis. *Nat. Commun.* **2011,** *469* (7331), 483–490.

4. http://www.newtbdrugs.org/pipeline.php, Accessed November 11, 2015.

5. U.S. Food and Drug Administration. http://www.fda.gov/NewsEvents/Newsroom/PressAnnouncements/ucm333695.htm **2012**, Accessed November 11, 2015.

6. European Medicines Agency. http://www.ema.europa.eu/ema/index.jsp?curl=pages/news_and_events/news/2013/11/news_detail_001972.jsp&mid=WC0b01ac058004d5c1 **2013**, Accessed November 11, 2015.

7. Cox, E.; Laessig, K., FDA approval of bedaquiline—the benefit-risk balance for drug-resistant tuberculosis. *N. Engl. J. Med.* **2014,** *371* (8), 689-691.

8. Domenech, P.; Reed, M. B.; Barry III, C. E., Contribution of the *Mycobacterium tuberculosis* MmpL protein family to virulence and drug resistance. *Infect. Immun.* **2005,** *73* (6), 3492-3501.

9. Owens, C. P.; Chim, N.; Graves, A. B.; Harmston, C. A.; Iniguez, A.; Contreras, H.; Liptak, M. D.; Goulding, C. W., The Mycobacterium tuberculosis secreted protein Rv0203 transfers heme to membrane proteins MmpL3 and MmpL11. *J Biol Chem.* **2013,** *288* (30), 21714-21728.

10. (a) Belisle, J. T.; Vissa, V. D.; Sievert, T.; Takayama, K.; Brennan, P. J.; Besra, G. S., Role of the major antigen of *Mycobacterium tuberculosis* in cell wall biogenesis. *Science* **1997,** *276*, 1420–1422; (b) Puech, V.; Guilhot, C.; Perez, E.; Tropis, M.; Armitige, L. Y.; Gicquel, B.; Daffe´ , M., Evidence for a partial redundancy of the fibronectin-binding proteins for the transfer of mycoloyl residues onto the cell wall arabinogalactan termini of *Mycobacterium tuberculosis*. *Mol. Microbiol.* **2002,** *44*, 1109–1122.

11. Kalscheuer, R.; Weinrick, B.; Veeraraghavan, U.; Besra, G. S.; Jacobs, W. R. J., Trehalose-recycling ABC transporter LpqY-SugA-SugB-SugC is essential for virulence of *Mycobacterium tuberculosis*. *Proc. Natl. Acad. Sci. U. S. A.* **2010,** *107* (50), 21761-21766.

12. Cole, S. T., Infectious diseases: transporter targeted in tuberculosis. *Nat. Chem. Biol.* **2012,** *8*, 326–327.

13. Tullius, M. V.; Harmston, C. A.; Owens, C. P.; Chim, N.; Morse, R. P.; McMath, L. M.; Iniguez, A.; Kimmey, J. M.; Sawaya, M. R.; Whitelegge, J. P.; Horwitz, M. A.; Goulding, C. W., Discovery and

characterization of a unique mycobacterial heme acquisition system. *Proc. Natl. Acad. Sci. U.S.A.* **2011,** *108* (12), 5051-5056.

14. Li, W.; Upadhyay, A.; Fontes, F. L.; North, E. J.; Wang, Y.; Crans, D. C.; Grzegorzewicz, A. E.; Jones, V.; Franzblau, S. G.; Lee, R. E.; Crick, D. C.; Jackson, M., Novel insights into the mechanism of inhibition of MmpL3, a target of multiple pharmacophores in *Mycobacterium tuberculosis*. *Antimicrob. Agents Chemother.* **2014,** *58* (11), 6413-6423.

15. Onajole, O. K.; Pieroni, M.; Tipparaju, S. K.; Lun, S.; Stec, J.; Chen, G.; Gunosewoyo, H.; Guo, H.; Ammerman, N. C.; Bishai, W. R.; Kozikowski, A. P., Preliminary structure-activity relationships and biological evaluation of novel antitubercular indolecarboxamide derivatives against drug-susceptible and drug-resistant *Mycobacterium tuberculosis* strains. *J. Med. Chem.* **2013,** *56* (10), 4093-4103.

16. Lun, S.; Guo, H.; Onajole, O. K.; Pieroni, M.; Gunosewoyo, H.; Chen, G.; Tipparaju, S. K.; Ammerman, N. C.; Kozikowski, A. P.; Bishai, W. R., Indoleamides are active against drug-resistant *Mycobacterium tuberculosis*. *Nat. Commun.* **2013,** *4*.

17. (a) Andrews, R. E.; Parks, L. W.; Spence, K. D., Some effects of douglas fir terpenes on certain microorganisms. *Appl Environ Microbiol.* **1980,** *40* (2), 301-304; (b) Sikkema, J.; de Bont, J. A.; Poolman, B., Mechanisms of membrane toxicity of hydrocarbons. *Microbiol Rev.* **1995,** *59* (2), 201–222.

18. Kondreddi RR, J. J., Rao SP, Lakshminarayana SB, Camacho LR, Rao R, Herve M, Bifani P, Ma NL, Kuhen K, Goh A, Chatterjee AK, Dick T, Diagana TT, Manjunatha UH, Smith PW., Design, synthesis, and biological evaluation of indole-2-carboxamides: a promising class of antituberculosis agents. *J. Med.Chem.* **2013,** *56* (21), 8849-8859.

19. Rao, S. P. S.; Lakshminarayana, S. B.; Kondreddi, R. R.; Herve, M.; Camacho, L. R.; Bifani, P.; Kalapala, S. K.; Jiricek, J.; Ma, N. L.; Tan, B. H.; Ng, S. H.; Nanjundappa, M.; Ravindran, S.; Seah, P. G.; Thayalan, P.; Lim, S. H.; Lee, B. H.; Goh, A.; Barnes, W. S.; Chen, Z.; Gagaring, K.; Chatterjee, A. K.; Pethe, K.; Kuhen, K.; Walker, J.; Feng, G.; Babu, S.; Zhang, L.; Blasco, F.; Beer, D.; Weaver, M.; Dartois, V.; Glynne, R.; Dick, T.; Smith, P. W.; Diagana, T. T.; Manjunatha, U. H., Indolcarboxamide is a

preclinical candidate for treating multidrug-resistant tuberculosis. *Sci. Transl. Med.* **2013,** *5* (214), 214ra168.

20. Chopra, S.; Matsuyama, K.; Tran, T.; Malerich, J. P.; Wan, B.; Franzblau, S. G.; Lun, S.; Guo, H.; Maiga, M. C.; Bishai, W. R.; Madrid, P. B., Evaluation of gyrase B as a drug target in *Mycobacterium tuberculosis*. *J. Antimicrob. Chemother.* **2012,** *67*, 415-421.

21. Ioerger, T. R.; Koo, S.; No, E.-G.; Chen, X.; Larsen, M. H.; Jacobs, W. R., Jr.; ; Pillay, M.; Sturm, A. W.; Sacchettini, J. C., Genome analysis of multi- and extensively-drug-resistant tuberculosis from KwaZulu-Natal, South Africa. *PLoS One* **2009,** *4*, e7778.

22. Lun, S.; Guo, H.; Onajole, O. K.; Pieroni, M.; Gunosewoyo, H.; Chen, G.; Tipparaju, S. K.; Ammerman, N. C.; Kozikowski, A. P.; Bishai, W. R., Indoleamides are active against drug-resistant Mycobacterium tuberculosis. *Nat Commun* **2013,** *4*, 2907.

23. (a) Bliss, C. I., The toxicity of poisons applied jointly. *Ann. Appl. Biol.* **1939,** *26*, 585-615; (b) Greco, W. R.; Bravo, G.; Parsons, J. C., The search for synergy: a critical review from a response surface perspective. *Pharmacol. Rev.* **1995,** *47*, 331-385.

24. (a) Branch, R. A.; Adedoyin, A.; Frye, R. F.; Wilson, J. W.; Romkes, M., *In vivo* modulation of CYP enzymes by quinidine and rifampin. *Clin Pharmacol Ther.* **2000,** *68*, 401–411; (b) Baciewicz, A. M.; Chrisman, C. R.; Finch, C. K.; Self, T. H., Update on rifampin, rifabutin, and rifapentine drug interactions. *Curr. Med. Res. Opin.* **2013,** *29*, 1–12.

25. Finch, C. K.; Chrisman, C. R.; Baciewicz, A. M.; Self, T. H., Rifampin and rifabutin drug interactions: an update. *Arch. Intern. Med.* **2002,** *162*, 985–992.

26. (a) Acosta, E. P.; Kendall, M. A.; Gerber, J. G.; Alston-Smith, B.; Koletar, S. L.; Zolopa, A. R.; Agarwala, S.; Child, M.; Bertz, R.; Hosey, L.; Haas, D. W., Effect of concomitantly administered rifampin on the pharmacokinetics and safety of atazanavir administered twice daily. *Antimicrob. Agents Chemother.* **2007,** *51*, 3104–3110; (b) Kirby, B. J.; Collier, A. C.; Kharasch, E. D.; Whittington, D.; Thummel, K. E.; Unadkat, J. D., Complex drug interactions of the HIV protease inhibitors 3: effect of

simultaneous or staggered dosing of digoxin and ritonavir, nelfinavir, rifampin, or bupropion. *Drug Metab. Dispos.* **2012,** *40*, 610–616.

27. Sennhauser, G.; Bukowska, M. A.; Briand, C.; Grütter, M. G., Crystal structure of the multidrug exporter MexB from *Pseudomonas aeruginosa*. *J. Mol. Biol.* **2009,** *389*, 134-145.

28. Pieroni, M.; Tipparaju, S.; Lun, S.; Song, Y.; Sturm, A. W.; Bishai, W. R.; Kozikowski, A. P., Pyrido[1,2-a]benzimidazole-based agents active against tuberculosis (TB), multidrug-resistant (MDR) TB and extensively drug-resistant (XDR) TB. *ChemMedChem.* **2011,** *6* (2), 334-342.

29. Laird, G. M.; Bullen, C. K.; Rosenbloom, D. I.; Martin, A. R.; Hill, A. L.; Durand, C. M.; Siliciano, J. D.; Siliciano, R. F., Ex vivo analysis identifies effective HIV-1 latency-reversing drug combinations. *J. Clin. Invest.* **2015,** *125*, 1901–1912.

Table of Contents graphic